Master's Thesis of Science
in Agricultural Biotechnology

Synthesis of carbon quantum dot from spent coffee ground exhibiting visible-light-driven antimicrobial activity against *Escherichia coli* O157:H7

Spent Coffee Ground (SCG)유래의 Carbon Quantum dot(CQD) 합성 및 광촉매 작용을 이용한 *Escherichia coli* O157:H7 저감화

February, 2023

The Graduate School
Seoul National University
Department of Agricultural Biotechnology

Jiyeong Kim

Synthesis of carbon quantum dot from spent coffee ground exhibiting visible-light-driven antimicrobial activity against *Escherichia coli* O157:H7

Advisor: Dong-Hyun Kang

Submitting a Master's Thesis of Science
in Agricultural Biotechnology

February 2023

The Graduate School
Seoul National University
Department of Agricultural Biotechnology

Jiyeong Kim

Confirming the master's thesis written by
Jiyeong Kim
February 2023

Chair	Young Jin Choi (seal)
Vice Chair	Dong-Hyun Kang (seal)
Examiner	Pahn Shick Chang (seal)

ABSTRACT

The aim of this study was to synthesize carbon quantum dot (CQD) exhibiting visible-light-driven (VLD) antimicrobial activity using spent coffee ground (SCG) as biomass. CQD was synthesized from SCG through microwave treatment. It was confirmed that typical CQD was synthesized through analysis of morphology (high-resolution transmission electron microscopy), size distribution (dynamic light scattering), and chemical structure (X-ray photoelectron spectroscopy). VLD antimicrobial activities of CQD synthesized from SCG against *Escherichia coli* O157:H7 were found to be increased as pH decreased. Fluorescence quantum yield (FLQY), band gap energy (Eg), and fluorescence lifetime as photodynamic properties of CQD related to VLD antimicrobial activity did not show any significant changes according to pH change. On the other hand, as pH decreased, negative zeta potential (mV) values of CQD and pathogenic bacteria gradually decreased. As a result, it was confirmed that CQD uptake into *E. coli* O157:H7 was gradually increased due to a decrease in repulsive force between them. It was confirmed that major reactive oxygen species (ROS) that contributed to the inactivation of *E. coli* O157:H7 was singlet oxygen. In addition, it was found that as pH decreased, activities of enzymes (superoxide dismutase and catalase) known to scavenge ROS in cells decreased. In the presence of CQD, when

visible light was applied, the amount of ROS generated inside the cell increased as the pH decreased. In addition, VLD antimicrobial activities of CQD were applied to the apple slices washing and significant ($P < 0.05$) reduction of *E. coli* O157:H7 occurred in both apple and liquid, and cross-contamination was also prevented. The activity of CQD was maintained after reuse for three consecutive treatment cycles, and there was no difference in activity by the date of manufacturing of CQD for four weeks. Results of this study suggest that it is advantageous to use CQD synthesized from SCG under acidic conditions and VLD antimicrobial activities can be applied to the fresh produce washing process. Further research is needed on a method for synthesizing CQD that is not affected by pH conditions.

Keywords: **Carbon quantum dot, visible-light-driven antimicrobial activity, *Escherichia coli* O157:H7, antibacterial activity, inactivation mechanism, fresh produce washing**

***Student Number*: 2021-27817**

CONTENTS

LIST OF TABLE

LIST OF FIGURES

I. INTRODUCTION

Globally, cross-contamination from minimally processed products such as fresh produce is considered a major risk factor for foodborne outbreaks (Yi, Huang, Young, & Nitin, 2020). Cross-contamination of minimally processed products during post-harvest processing such as washing treatment is usually caused by the transfer from pathogens of contaminated produce to uncontaminated produce in the washing water (Ding & Tikekar, 2020). Therefore, it is important to reduce the risk of cross-contamination by controlling foodborne pathogens in the washing water to suppress their spread. However, conventional water disinfection methods such as chemical sanitizing agents and ultraviolet (UV) treatment have unavoidable limitations such as the formation of harmful disinfection byproducts, not being eco-friendly, and cost problems such as energy consumption (Zhang, Li, Shuai, Shen, Xiong, & Wang, 2019). In this regard, there is a need to explore next-generation water disinfectant technology that is safe, highly efficient, cost-effective, eco-friendly, and sustainable.

Semiconductor photocatalytic disinfection technology that utilizes visible light of natural light such as sunlight and indoor light is spotlighted as a promising technology because it is energy efficient without forming harmful

by-products with characteristics of being reusable (Shi, Wang, Wang, Hu, Fan, & Tang, 2021; C. Zhang et al., 2018). In this technology, electron (e-)-hole (h+) pairs created on the surface of a semiconductor material by light energy can convert water and oxygen into reactive oxygen species (ROS) under ambient conditions, thereby exerting a control effect on microorganisms (Tzeng et al., 2021). Because ROS are highly reactive that can non-specifically cause damage to essential cellular components, they have a strong control effect on a wide range of microorganisms without inducing resistance (Tavares et al., 2010; Xia, Shen, Huang, Wang, Yu, & Wong, 2015).

Carbon quantum dot (CQD), a new class of carbon-based nanoparticles with outstanding properties such as high stability, low toxicity, good biocompatibility, high water solubility, and low manufacturing cost, has a high potential for use in photocatalytic technology (Abd Rani, Ng, Ng, & Mahmoudi, 2020; T. Wang et al., 2018). In particular, while conventional nano-sized semiconductor photosensitizers require UV light to be active, CQD can be activated in the visible light spectrum to exhibit antimicrobial activities against a wide range of microorganisms such as bacteria, antibiotic-resistant pathogens, and viruses (Dong et al., 2018; Dong, Liang, Meziani, Sun, & Yang, 2020; Dong, Overton, Tang, Darby, Sun, & Yang, 2021).

Worldwide, about one-third of food produced for human consumption, which is equivalent to 1.3 billion tons per year, is lost or wasted. Such food waste occurs at all stages of the food supply chain from production to consumption (Ebikade, Sadula, Gupta, & Vlachos, 2021; Vilariño, Franco, & Quarrington, 2017). Most of such waste is directly thrown away, landfilled, or burned, which can cause serious environmental problems as well as economic loss due to additional treatment or waste of resources (Babbar & Oberoi, 2014; C. Kang, Huang, Yang, Yan, & Chen, 2020). Based on these facts, devising a sustainable method through an upcycling strategy that can convert food waste into useful materials is urgently needed. It has been demonstrated that CQD can be synthesized from any starting materials containing carbon. Food waste is a natural organic carbon source, meaning that it can be utilized for synthesizing CQD (C. Kang et al., 2020; Yi et al., 2020). Utilizing food waste as a synthetic material for CQD not only helps us solve inherent problems of food waste, but also has the advantages of using a very good synthetic material because food waste is sustainable, eco-friendly, inexpensive, easy to obtain, and abundant as a carbon source (Meng, Bai, Wang, Liu, Lu, & Yang, 2019; Shahraki, Ahmad, & Bushra, 2022).

It is known that various properties of CQD can be changed by doping, through which elements other than carbon can be additionally introduced into

CQD to change the carbon framework or surface chemical structure (Kou, Jiang, Park, & Meng, 2020; Miao, Liang, Zhu, Yang, Zhao, & Kong, 2020). Food waste is a material that has abundant proteins. Nitrogen and sulfur also exist in large proportions in amino acids of proteins in addition to carbon (Prandi et al., 2019). Thus, when synthesizing CQD using food waste, N and S can be doped. However, since the composition and content of amino acids vary by food type (Gardner, Hartle, Garrett, Offringa, & Wasserman, 2019), CQD with different characteristics will be synthesized depending on the type of food by-products. It is known that the activity of CQD is increased when the content of amino acid is increased while the ratio of amino acid containing sulfur is decreased (J.-W. Kang & Kang, 2021). About 50% of spent coffee ground (SCG), a by-product discarded after coffee extraction, is in the form of (hemi)-cellulose, which has abundant carbon. During the extraction process, only about 33% of the protein is extracted. The rest remains as insoluble residues due to denaturation and so on. Thus, SCG has a high amino acid content (Campos-Vega, Loarca-Pina, Vergara-Castañeda, & Oomah, 2015). According to previous research (Martinez-Saez et al., 2017), cysteine and methionine as amino acids containing S exist in very low proportions (about 0.4%) in SCG. Thus, CQD synthesized using SCG is expected to show excellent VLD antimicrobial activity. Furthermore, it is known that coffee

beans have similar protein contents even if coffee species and roasting methods are different, meaning that CQD with relatively constant characteristics can be synthesized using SCG (Casal, Mendes, Oliveira, & Ferreira, 2005; Cruz et al., 2012; Martinez-Saez et al., 2017). For these reasons, SCG is considered a suitable raw material for synthesizing CQD with VLD antimicrobial activity.

In this study, CQD was synthesized using SCG. The possibility of applying COD as visible-light-driven catalytic reaction-based water disinfectants was verified. For this purpose, antimicrobial effects of SCG-derived CQD on *Escherichia coli* O157:H7 under visible light irradiation were investigated. It is known that CQD can change their properties such as fluorescence intensity (Song, Quan, Xu, Liu, Cui, & Liu, 2016) (Lei, Hsieh, & Liu, 2019), bacterial growth inhibition activity (P. Li et al., 2020), and catalytic activity (Tripathi et al., 2020) depending on the pH condition. Thus, we evaluated VLD antimicrobial activities according to pH conditions. The mechanism involved in the change of activity by pH was further investigated.

Fresh produce mostly contains organic matter, and in the case of chlorine, the inactivation effect may be reduced if it reacts with organic matter (Shen, Luo, Nou, Wang, & Millner, 2013). Therefore, apple samples were used to determine whether organic matter affects VLD antimicrobial inactivation of *E.*

coli O157:H7 which is a major pathogen that can be found in fresh produces (Heiman, Mody, Johnson, Griffin, & Gould, 2015). To investigate the applicability of CQD as a sanitation agent, reusability and activity change over time were also investigated.

To sum up, this study was examined to investigate the antimicrobial activity of CQD in presence of visible light and the applicability of VLD antimicrobial activities of CQD to the washing process of fresh produce.

II. MATERIALS AND METHODS

2.1. Synthesis of CQD

SCG (Arabica) was used as a source of carbon for the synthesis of CQD. It was bought from a local cafeteria in Seoul, South Korea. SCG (20 g) was added in 30 mL of ultrapure distilled water in a 250 mL Erlenmeyer flask and incubated in a 70°C water bath for 10 min. The completely dissolved solution was treated in a domestic microwave (700 W) for 5 min at maximum power. It was then allowed to cool to room temperature (22 ± 2°C). Then 100 mL of ultrapure distilled water was added to the reacted solid product. After incubating in a water bath for 30 min at 70°C, the solution was centrifuged at 10,000 g for 20 min to obtain supernatant. The supernatant was filtered with a syringe filter (0.22 μm). After that, dialysis membrane (MWCO 500 – 1000 Da) was rinsed in ultrapure distilled water and used to dialyze the filtered solution. Dialysis membrane was soaked against ultrapure distilled water for 3 days, during which the ultrapure distilled water was changed every 24 h. The dialyzed solution was freeze-dried to obtain dried CQD.

2.2. Characterization

The synthesized CQD from SCG was characterized using various measuring instruments. Morphologies of particles were observed with a 200 kV transmission electron microscope (TEM) (JEM-F200, JEOL, Japan). Particle size distribution of CQD was analyzed through dynamic light scattering (DLS) using a Zetasizer Nano ZS (Malvern Instruments Ltd., Malvern, UK). Surface chemical structures of CQD were determined using X-ray photoelectron spectroscopy (XPS, K-alpha, Thermo Scientific, UK). Photoluminescence (PL) lifetime of CQD was determined using a time-correlated single-photon counting (TCSPC) system (PicoHarp300, PicoQuant GmbH, Germany). Exponential fitting for PL decays was achieved using a Symphotime-64 software (Ver. 2.2).

2.3. Bacterial culture and inoculum preparation

Three strains (ATCC 43890, 43889, and 35150) of *E. coli* O157:H7 were obtained from the Food Safety Engineering Laboratory at Seoul National University (Seoul, Republic of Korea) for this study. Stock cultures stored at −80°C were streaked onto tryptic soy agar (TSA; Difco, BD) plates, incubated at 37°C for 24 h, and kept in a refrigerator at 4°C as working culture. Prepared strains were cultured individually in 5 mL of tryptic soy broth (Difco, BD,

Sparks, MD) at 37°C for 24 h. Cultured cells were collected by centrifugation at 4,000 rpm for 20 min. The pellet was washed with phosphate buffer saline (PBS) and re-suspended with PBS. Resuspended solution was comprised of approximately 10^9 – 10^{10} CFU/mL. This solution was used in this study.

2.4. Antimicrobial effect of CQD under visible light irradiation

In this study, xenon lamp (100 W) equipped with a solar simulator (DXFL100, DTX Inc., Siheung, South Korea) and a UV cut-off lens ($\lambda < 400$) was used to provide visible light. After CQD at a concentration of 1 mg/mL was added to PBS, pH values were adjusted by adding hydrochloric acid (HCl, 0.1 M). And then, 5.0 mL of each solution was placed in a Petri dish (35 mm × 15 mm). After, 0.1 mL of the inoculum was added to each solution and lid was closed. The vertical distance between the Petri dish and the lamp was 5 cm. The integral light intensity was measured with a fiber optic spectrometer (AvaSpec-ULS2048; Avantes, Eerbeek, Netherlands) with the range set at 400 – 800 nm for the sample surface. The integral light intensity was 7.8 mW/cm^2. Doses of treated samples with visible light were 0 – 84.24 J/cm^2 (0 – 180 min) at room temperature (22 ± 2°C). During treatment, samples were mixed via pipetting at 10 min intervals. After each treatment, 1 ml of treated sample was

transferred to 9 ml of 0.2% peptone water (Difco) and serially diluted ten-fold. Then 0.1 ml aliquots of dilutions were spread onto Sorbitol MacConkey Agar (SMAC, Difco) plates for enumeration of *E. coli* O157:H7. All plates were incubated at 37°C for 24 h. Colonies on the media were enumerated and calculated as log10 CFU/mL. Using the same procedure, enumeration was conducted for dark control which included CQD without visible light treatment and light control with only visible light treatment without CQD.

2.5. Fluorescence Quantum yield (FLQY) measurement

To measure fluorescence quantum yields, an established comparative method was applied which uses known fluorescence standard sample. Absorbance values of the sample and the standard at the same excitation wavelength were matched. Then, the quantum yield values of the sample are obtained using the quantum yield values of the known standard. In this study, quinine sulfate (Sigma-Aldrich, St. Louis, MO, USA) was dissolved in 0.1 M H_2SO_4 and used as reference standard (FLQY: 54%). PL spectra of CQD dissolved in PBS with pH adjusted to 2.5, 3.0, and 4.0 with HCl and quinine sulfate dissolved in 0.1 M H_2SO_4 were obtained at an excitation wavelength of 360 nm in 10 mm path length fluorescence cuvettes. Integrated PL

intensities were derived from the spectra. Absorbance values of each CQD and reference standard samples were maintained below 0.1 to reduce the effect of re-absorption. A plot composed of the integrated PL intensity and its corresponding absorbance value was obtained. The FLQY (%) was calculated as follows:

$$FLQYx(\%) = FLQYs(Gradx/Grads)(\eta s/\eta x)$$

where subscripts s and x denoted standard (quinine sulfate) and test (CQD with different pH) respectively, Grad was the slope in the equation, η was the refractive index of the solvent, and ηx and ηs were both 1.33.

2.6. Band gap energy determination

Tauc modeling was applied to determine the band gap energy (Eg) of CQD from SCG. Tauc modeling equation was as follows:

$$\alpha h\nu = A(h\nu - E_g)^n$$

where A is a constant, α is the absorption coefficient, hν is the photon energy, and n = 1/2 and 2 are for direct and indirect allowed transitions, respectively (Tyutrin, Wang, & Martynovich, 2022; Y. Yang et al., 2017).

Considering CQD is a direct allowed type of transition semiconductor, the $(\alpha h\nu)^2$ versus hν plot (Tauc plot) was obtained using UV–vis absorption

spectrum of C-dots. The band gap energy was determined by calculating the intercept of the incident photon energy axis by adding the straight part of the plot (H.-X. Wang et al., 2015).

2.7. Measurement of surface charge

Surface charges of bacterial cells and CQD from SCG were evaluated by measuring zeta potentials of microorganisms and CQD at different pH values of 2.5, 3.0, and 4.0. Bacterial cell suspensions were centrifuged at 4,000 g for 20 min. Collected cell pellets were re-suspended in 10 mL of PBS. Pathogen suspension was 10-fold diluted in sterile PBS buffer and pH was adjusted with 0.1 M HCl. CQD solution was prepared at a concentration of 1 mg/mL by adding 0.1 M HCl to set the pH. Zeta potential measurement was conducted with a Zetasizer Nano ZS (Malvern Instruments Ltd., Malvern, UK).

2.8. CQD uptake

To evaluate the degree of CQD uptake by bacterial cells depending on pH conditions, cells of *E. coli* O157:H7 were incubated with PBS containing 1 mg/ml CQD adjusted to pH 2.5, 3.0, and 4.0, respectively, at an optical

density of 1.5 at 600 nm for 3 h at room temperature (22 ± 2°C). After incubation, bacterial cells were centrifuged at 10,000 g for 10 min and washed twice with PBS to remove CQD not uptaken. Final pelleted cells were re-suspended with PBS. Fluorescent intensities of cell suspension were measured with a spectrofluorophotometer (Spectramax M2e; Molecular Devices, Sunnyvale, CA, USA) at excitation/emission wavelengths of 360 nm/450 nm. Cell suspension not incubated with CQD solution was used as control.

2.9. ROS scavenger

Solutions with or without 1 mg/mL CQD in PBS adjusted to pH 2.5, 3.0, and 4.0 were used with ROS scavengers. The antimicrobial effects were verified at 28.8 J/cm^2 with 5 mM sodium pyruvate, 50 mM mannitol, 5 mM sodium azide, and 5 mM Trion. For the experiment, 0.1 mL of the inoculum was added to each solution with each scavenger and lid was closed. After treatment, each sample was serially diluted ten-fold. Then diluted sample was plated for enumeration.

2.10. ROS defense enzyme

Activities of superoxide dismutase (SOD) and catalase (CAT) as ROS scavenging enzymes targeting O_2^- and H_2O_2, respectively, were measured. *E.*

coli O157:H7 cells were incubated with PBS adjusted to pH 2.5, 3.0, and 4.0 at an optical density of 1.5 at 600 nm for 3 h. After incubation, cells were centrifuged at 10,000 g for 10 min and washed twice with PBS. Final pelleted cells were re-suspended with PBS. Re-suspended cells were disrupted with a sonicator (10 s on and 10 s off, six times) in an ice bath and centrifuged at 10,000 g for 10 min at 4 °C to collect scavenging enzymes remaining in the supernatant. SOD and CAT activities (%) were measured using an SOD assay kit -WST (Sigma-Aldrich) and an Amplex Red CAT assay kit (Invitrogen, Carlsbad, CA, USA), respectively, following each manufacturer's instructions.

2.11. Measurement of intracellular ROS (iROS) generation and cell membrane damage

To measure the degree of intracellular ROS generation and structural damage, cellular dye 5-(and-6)-chloromethyl-2',7'-dichlorodihydrofluorescein diacetate (CM-H2DCFDA; Molecular Probes, Thermo Fisher Scientific) and propidium iodide (PI; Sigma Aldrich) were used. For the experiment, cells of *E. coli* O157:H7 with an optical density of 0.3 at 600 nm in PBS adjusted to pH 2.5, 3.0, and 4.0 with or without 1 mg/ml of CQD were treated with visible light and centrifuged at 10,000 g for 10 min followed by washing twice with

PBS. Final cell pellets were incubated with CM-H2DCFDA or PI, dye at a concentration of 5 or 2.9 μM, respectively, for 10 min. After incubation, cells were harvested by centrifugation at 10,000 g for 10 min followed by washing twice with PBS. Fluorescence was measured with a spectrophotometer at excitation/emission wavelengths of 495/520 and 493/630 nm for iROS generation, PI assay, respectively. Using obtained florescent signals, each value was determined as follows: [(Fluorescence value of visible light treated cells) – (Fluorescence value of dark-treated cells).

For the experiment of lipid peroxidation, cells of *E. coli* O157:H7 in PBS adjusted to pH 2.5, 3.0, and 4.0 with or without 1 mg/ml of CQD were treated with visible light. To measure the degree of lipid peroxidation, thiobarbituric acid reactive substances assay (Tbars, cell biolabs) was used. 100 μm treated samples were transferred to microcentrifuge tubes. SDS lysis solution was put into samples and incubated for 5 min at room temperature. 5.2 mg/mL solution of thiobarbituric acid (TBA) reagent was added and incubated at 95 °C for 60 min. After incubation, microcentrifuge tubes were transferred and incubated in ice bath for 5 min. Samples were centrifuged at 3,000 g for 15 min and supernatant was used to measure fluorescence with a spectrophotometer at excitation/emission wavelengths of 540/590 nm. Using obtained florescent

signals, each value was determined as follows: [(Fluorescence value of visible light treated cells) – (Fluorescence value of dark-treated cells).

2.12. Application of VLD antimicrobial activities of CQD on apple washing process

The VLD antimicrobial activities of CQD were applied to fresh produce washing. The reusability of CQD and changes in activity over time were measured.

2.12.1. Application on apple washing produce

VLD antimicrobial activities of CQD on the washing process were examined. Fresh apples were purchased at a local market, stored at 4℃, and used within a week. Apple slices were prepared of 1 x 1 cm^2. CQD solutions at a concentration of 1, 3, and 5 mg/mL each were prepared in PBS and adjusted to pH value of 2.5 with HCl. 20 mL of CQD solution was transferred to petri dish (90 mm × 15 mm). 10 μl bacterial of *E. coli* O157:H7 was inoculated on apple slices by spotting with a micropipette at 7 to 10 locations and dried for 1 h in the laminar flow biosafety hood at room temperature

(22 ± 2°C) for sufficient attachment of bacteria. To evaluate the degree of cross-contamination inhibition, uninoculated samples were prepared, too. Four inoculated and uninoculated samples were put in CQD solution, respectively. At this time, one treatment group was irradiated with visible light, and the other was placed in a dark state. Each inoculated and uninoculated sample was taken out every hour. As a control, prepared apple slices were put in PBS without light and taken out every hour.

After treatment, samples were individually transferred into sterile stomacher bags (Labplas Inc., Sainte-Julie, QC, Canada) containing 50 ml of PW and homogenized for 2 min with a stomacher (Easy Mix; AES Chemunex, Rennes, France). Simultaneously, CQD solution in which samples were immersed was withdrawn to enumerate surviving bacteria after treatment. After homogenization or sampling, 1 ml aliquots of treated samples or CQD solution suspensions were 10-fold serially diluted and spread-plated. The enumerated bacterial populations were expressed as Log CFU/sample or Log CFU/20 mL.

2.12.2. Reusability of VLD antimicrobial activities of CQD on apple washing process

To evaluate the reusability of CQD, three consecutive cycles of VLD treatment of CQD were performed. Two apple slices were prepared as described above. CQD concentration was fixed at 3 mg/mL and pH value was adjusted to 2.5. Samples were transferred to 20 mL CQD solution inside petri dish (90 mm × 15 mm). Samples were taken out after 3 and 4 hours, respectively. CQD solution were taken after 3 and 4 hours, respectively. After treatment, the remaining sample was subjected and filtered using a 0.22 μm syringe filter (Milllipore). Two apple slices were then put into a filtered CQD solution and VLD treatment of CQD was implemented in the same process. The treatment was conducted under the same conditions and procedures throughout the whole three cycles.

2.12.3. Evaluation of changes of CQD activity with temperature and storage time

To examine the changes of CQD activity with temperature and storage time, VLD treatment of CQD was conducted by the manufacturing date of the CQD stock solution. After CQD was synthesized, the stock solution was prepared immediately. Prepared stock solutions were stored at 4°C. Experiments were conducted on the 3rd day and, 1st, 2nd, and 4th weeks from

the date of manufacture of the CQD stock solution. Two apple slices were prepared as described above. CQD solution was prepared with a concentration of 3 mg/mL and pH value was adjusted to 2.5. Samples were transferred to 20 mL CQD solution inside petri dish (90 mm × 15 mm). Samples were taken out after 3 and 4 hours, respectively. CQD solution was taken after 3 and 4 hours, respectively. The treatment was conducted under the same conditions and procedures throughout the whole treatment.

2.13. Statistical analysis

All data were obtained from three independent replicates. Data were analyzed using analysis of variance (ANOVA) and the least significant difference (LSD) t-test using the Statistical Analysis System (SAS) Version 9.4 (SAS Institute Inc., Cary, NC, USA). A probability level of $P < 0.05$ was used to determine significant differences.

III. RESULTS AND DISCUSSIONS

3.1. Characterization of CQD synthesized from SCG

Fig. 1 shows morphology and particle size distribution measured by HRTEM imaging and DSL techniques of CQD, respectively. HRTEM (Fig. 1A) image showed a small, uniform, and spherical shape structure of the CQD with lattice fringes of 0.29 nm, which might ascribe to the sp^2 graphitic with crystalline structure (Lu et al., 2019). Fig. 1B shows the size distribution of CQD synthesized from SCG with a narrow size distribution ranging from 0.6 to 22 nm. The average diameter of CQD was 11.2 nm. A previous study (Alam, Park, Ghouri, Park, & Kim, 2015) has synthesized CQD from cabbage using a hydrothermal reactor with a size ranging from 2 to 6 nm which is relatively smaller than the CQD synthesized from SCG. Another study (Prasannan & Imae, 2013) has performed hydrothermal carbonization, resulting in a size distribution of 2−7 nm. However, other reports on CQD from onions with autoclave and soy milk from hydrothermal have revealed that CQD has a size distribution in the range of 7–25 nm and 13–40 nm, respectively (Bandi, Gangapuram, Dadigala, Eslavath, Singh, & Guttena, 2016; Zhu, Zhai, & Dong, 2012), similar to the tendency of results of the present study. From various

tendencies of its sizes, it can be interpreted that the size of CQD can be various depending on raw materials and extraction methods.

For the purpose of understanding the surface state and contents of CQD, XPS analysis was conducted (Fig. 2). Through XPS analysis, the surface chemistry of CQD could be confirmed (Jansen & Van Bekkum, 1995). CQD from SCG contained C1s and N1s peaks. The atomic ratio of C1s: N1s: S2p elements was 88.68: 11.10: 0.22. High-resolution C1s spectra revealed that CQD from SCG had peaks at 284.46, 285.83, 287.58, 288.43, and 292.42 eV related to C=C, C-N, C-O, C-C, and C-O-H, respectively (Ameen, Ward, Short, Beamson, & Briggs, 1993; Jansen et al., 1995; Y.-R. Liu et al., 2017; Liu, Zhou, Li, Deng, & Zhang, 2017; Oakley & Klobukowski, 2018). High-resolution spectra of N1s showed peaks at 399.07, 399.69, 398.49, and 400.55 eV corresponding to -N=, C-N, pyridinic N, and C-N-H, respectively (Chen et al., 2021; Kavaklı, Kavaklı, Seko, Tamada, & Güven, 2016; Y. Li, Liu, Zhu, Shen, Liu, & You, 2020; Yu et al., 2020). These results revealed that CQD from SCG contained mainly C, O, and N. It was confirmed that nitrogen doped on the surface of CQD can act as a passivating agent with oxygen (Alam et al., 2015). In particular, it has been demonstrated that N doping can increase the VLD antimicrobial activity of CQD (J.-W. Kang et al., 2021). This means that

CQD synthesized from SCG has suitable properties for water disinfectant using VLD catalytic reaction.

(A)

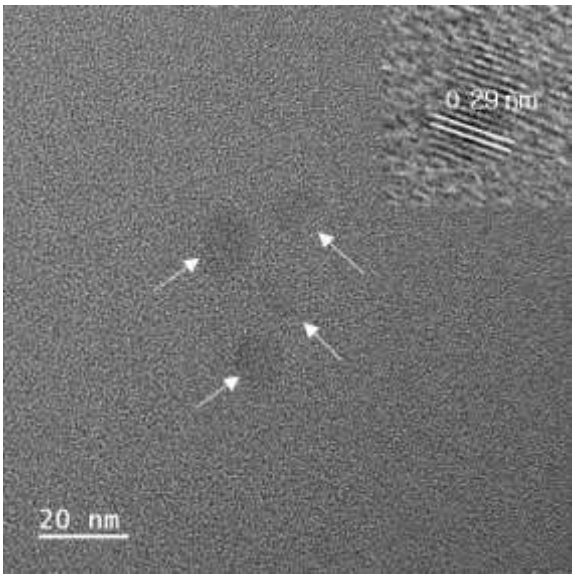

(B)

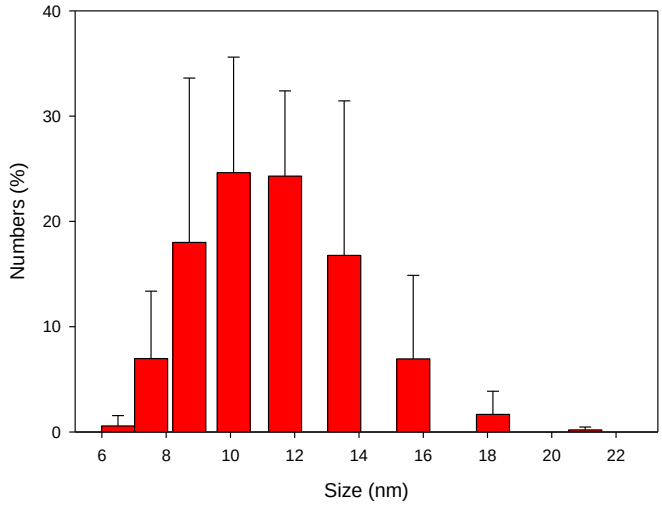

Fig 1 (A) High-resolution transmission electron microscopy (HRTEM) image and (B) size distribution (%) of carbon quantum dot (CQD) synthesized from spent coffee ground (SCG).

(A)

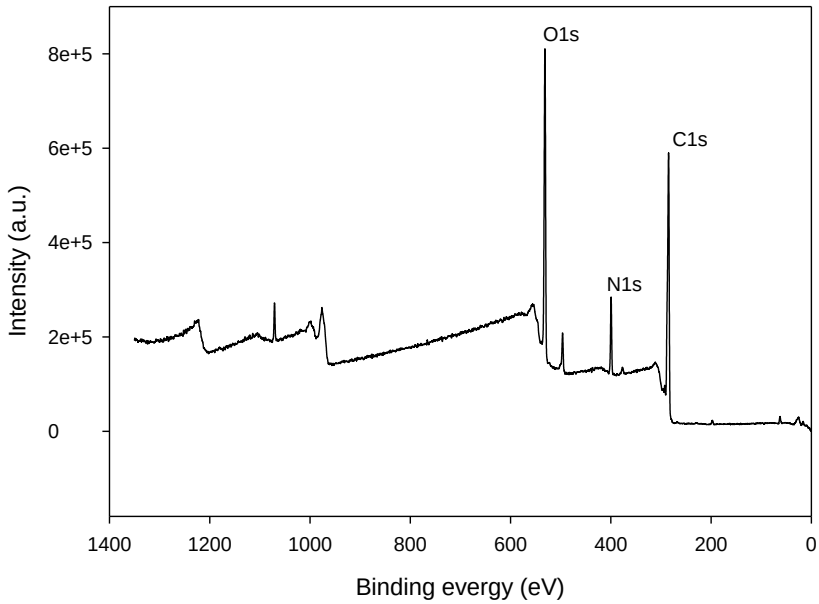
O1s
C1s
N1s
8e+5
6e+5
4e+5
2e+5
0
Intensity (a.u.)
1400
1200
1000
800
600
400
200
0
Binding evergy (eV)

(B)

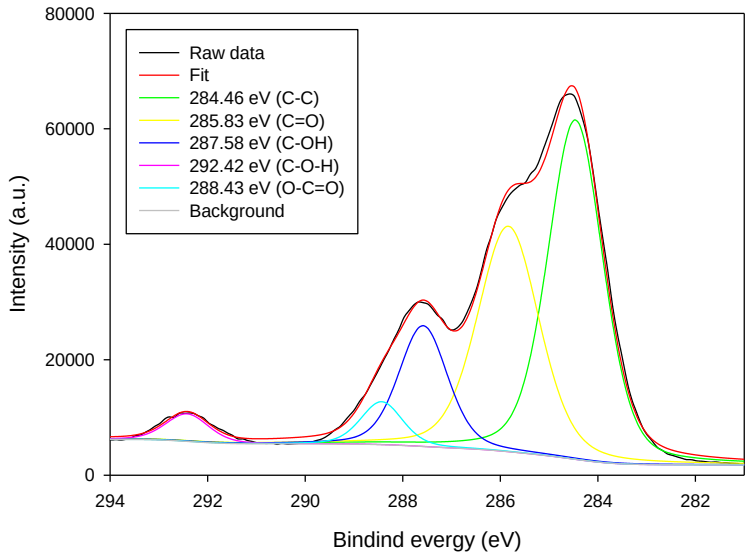
Raw data
Fit
284.46 eV (C-C)
285.83 eV (C=O)
287.58 eV (C-OH)
292.42 eV (C-O-H)
288.43 eV (O-C=O)
Background
80000
60000
40000
20000
0
Intensity (a.u.)
294
292
290
288
286
284
282
Bindind evergy (eV)

(C)

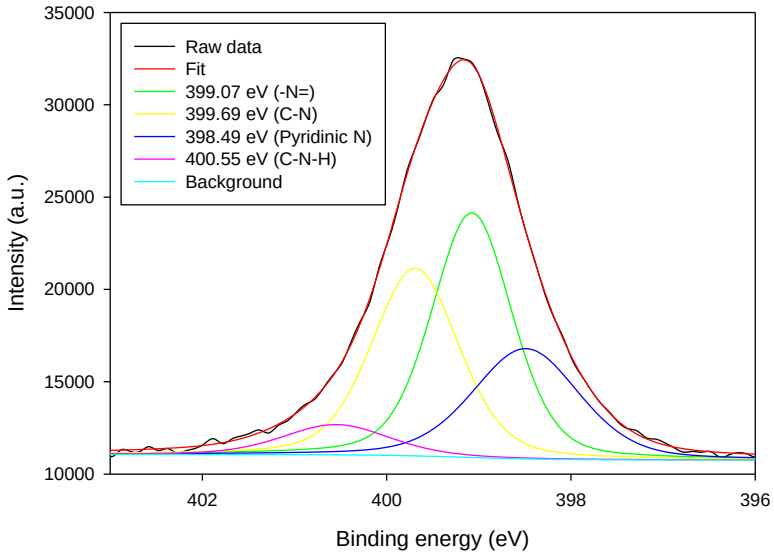

Fig 2 X-ray photoelectron spectroscopy (XPS) spectra of carbon quantum dot (CQD) synthesized from spent coffee ground (SCG): (A) Survey spectrum, (B) High resolution C1s spectra, and (C) High resolution N1s spectra.

3.2. Comparison of VLD antimicrobial activities of CQD synthesized from SCG at different pH conditions

To evaluate the applicability of CQD synthesized from SCG as a VLD catalytic reaction-based water disinfectant, its antimicrobial activities against *E. coli* O157:H7 under visible light treatment were investigated. Table 1 shows the results of antimicrobial activities of CQD synthesized from SCG under visible light irradiation depending on different pH conditions against *E. coli* O157:H7 in PBS. Initial bacterial concentrations of *E. coli* O157:H7 in PBS with 1 mg/mL of CQD at pH 2.5, 3.0, and 4.0 were 7.36, 7.46, and 7.43 log CFU/mL, respectively. Initial concentrations of *E. coli* O157:H7 in PBS without CQD at pH 2.5, 3.0, and 4.0 were 7.20, 7.71, and 7.30 log CFU/mL, respectively. Regardless of the presence or absence of CQD, significant ($P < 0.05$) reduction was observed for *E. coli* O157:H7 from 14.4 J/cm^2 (30 min treatment) from 28.08 J/cm^2 (1 h treatment) in the dark state at pH 2.5. There were no significant differences ($P > 0.05$) in the reduction between with and without CQD. At pH 3.0 and 4.0, there was no significant ($P > 0.05$) reduction for *E. coli* O157:H7 during 84.24 J/cm^2 treatment in the dark state. Since the acidic condition affected reduction results, values were processed by subtracting the reduction value after light treatment by the reduction value in the dark state. This was expressed as Light – Dark to only compare the VLD

antimicrobial effect. The reduction value of Light – Dark in the presence of CQD (1 mg/mL) was significantly ($P < 0.05$) greater than the reduction value of Light – Dark in the absence of CQD, meaning that CQD derived from SCG exhibited VLD antimicrobial activity. Although several studies have reported that CQD exhibits an antimicrobial activity through a catalytic reaction under visible light (Al Awak, Wang, Wang, Tang, Sun, & Yang, 2017; Dong et al., 2018; J.-W. Kang et al., 2021; Meziani et al., 2016; Rabe et al., 2019). The present study is the first to verify that CQD synthesized using biomass exhibits VLD antimicrobial activity. Moreover, reduction values of Light – Dark showed that as the pH decreased, the VLD antimicrobial activity of CQD increased. In particular, at pH 4, the VLD antimicrobial activity of CQD did not appear during treatment with 84.24 J/cm^2 of visible light. The same trend was observed under neutral conditions (pH 7.0) and alkaline conditions (pH 11.0) (data not shown). This means that VDL antimicrobial activity of CQD synthesized from SCG is more effective when it is utilized under low pH conditions.

Table 1 Log reductions (Log CFU/mL) of *E. coli* O157:H7 in phosphate buffer saline in the presence of (A) 1 mg/mL of carbon quantum dot (CQD) synthesized from spent coffee ground (SCG) or (B) absence of CQD under visible light or dark treatment

(A)

pH	Treatment	Log reduction (Log CFU/ml)			
		Dose (J/cm^2)			
		14.4	28.8	57.6	86.4
2.5	Dark	0.96 ± 0.09 Aa	2.13 ± 0.70 Ba	-	-
	Light	3.31 ± 0.44 Ab	> 6.53 ± 0.34 Bb	-	-
	Light - Dark	2.35 ± 0.36 A	> 4.41 ± 0.97 B		
3.0	Dark	-	0.19 ± 0.19 Aa	0.40 ± 0.35 Aa	0.61 ± 0.17 Aa
	Light	-	2.83 ± 0.96 Ab	4.53 ± 0.97 Bb	6.02 ± 0.63 Cb
	Light - Dark	-	2.64 ± 0.83 A	4.14 ± .61 B	5.41 ± 0.55 C
4.0	Dark	-	0.08 ± 0.07 Aa	0.16 ± 0.03 Aa	0.14 ± 0.13 Aa
	Light	-	0.21 ± 0.05 Aa	0.28 ± 0.14 Aa	0.36 ± 0.21 Aa
	Light - Dark	-	0.12 ± 0.12 A	0.11 ± 0.10 A	0.22 ± 0.08 A

(B)

Log reduction (Log CFU/ml)					
pH	Treatment	Dose (J/cm^2)			
		14.04	28.8	57.6	86.4
2.5	Dark	1.04 ± 0.13 Aa	2.33 ± 0.41 Ba	-	
	Light	1.95 ± 0.39 Ab	3.25 ± 0.19 Bb	-	
	Light - Dark	0.90 ± 0.27 A	0.91 ± 0.22 A		
3.0	Dark	-	0.22 ± 0.15 Aa	0.21 ± 0.17 Aa	0.35 ± 0.10 Aa
	Light	-	0.38 ± 0.27 Aa	0.87 ± 0.24 Aa	1.52 ± 0.19 Bb
	Light - Dark	-	0.16 ± 0.16 A	0.66 ± 0.10 B	1.18 ± 0.28 C
4.0	Dark	-	0.05 ± 0.05 Aa	0.03 ± 0.07 Aa	0.01 ± 0.19 Aa
	Light	-	0.09 ± 0.20 Aa	0.45 ± 0.18 Aa	0.30 ± 0.11 Aa
	Light - Dark	-	0.04 ± 0.17 A	0.42 ± 0.23 A	0.29 ± 0.10 A

Values are presented as means ± standard deviations from three independent replications.
Means with different capital letters within the same row are significantly different ($P < 0.05$).
Means with different lowercase letters within the same column are significantly different ($P < 0.05$).

3.3. Change in photodynamic properties of CQD synthesized from SCG at different pH conditions

The quantum yield of fluorescence is the ratio of the number of photons emitted through fluorescence to the number of photons absorbed (Grabolle, Spieles, Lesnyak, Gaponik, Eychmüller, & Resch-Genger, 2009). The higher the QY, the higher the conversion rate to the photo-excitation state for the same incident light energy and the greater the antimicrobial activity. Indeed, it has been reported that the VLD antimicrobial activity of CQD has a proportional relationship with its QY (Al Awak et al., 2017; J.-W. Kang et al., 2021). Furthermore, several studies have reported that the QY of CQD can change according to pH conditions (Ando & Akiyama, 2010; Meierhofer et al., 2020; G. Yang, Wan, Su, Zeng, & Tang, 2016). In addition, bandgap energy, which indicates the minimum energy level required to activate a semiconductor material, can affect the VLD antimicrobial activity of CQD. At lower bandgap energy of CQD, more visible light energy can be harvested, leading to a higher conversion rate to the photo-excited state (J.-W. Kang et al., 2021; Y. Zhang et al., 2018). Lei et al. (2019) have reported that the band gap energy of CQD changes according to pH conditions (Lei et al., 2019). Together with the above two factors, it was also revealed that the fluorescence lifetime of CQD was related to the VLD antimicrobial activity because the

longer the fluorescence lifetime, the longer the photo-excited state of CQD could be maintained. Thus, the rate of return to the ground state without reacting was reduced (J.-W. Kang et al., 2021; Y. Zhang et al., 2018). Based on these facts, it was hypothesized that the change in the VLD antimicrobial activity of CQD synthesized from SCG according to pH conditions was due to changes in the above-described factors (QY, bandgap energy, fluorescence lifetime). Thus, each factor was measured at different pH conditions (pH 2.5, 3.0, and 4.0). Contrary to expectation, it was found that QY (Fig. 3), bandgap energy (Fig. 4), and fluorescence lifetime (Fig. 5) of CQD synthesized from SCG did not show any significant ($P > 0.05$) changes when pH conditions were changed. This indicates that the cause of the change in the VLD antimicrobial activity of CQD derived from SCG according to pH change was not due to changes in internal factors (photodynamic property), but due to other external factors.

(A)

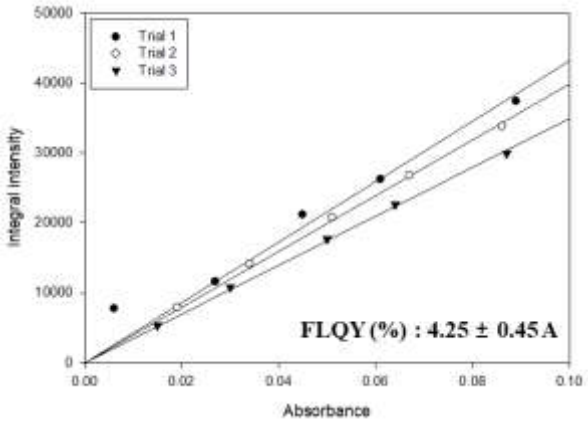
Trial 1
Trial 2
Trial 3
Integral intensity
Absorbance
FLQY (%) : 4.25 ± 0.45 A

(B)

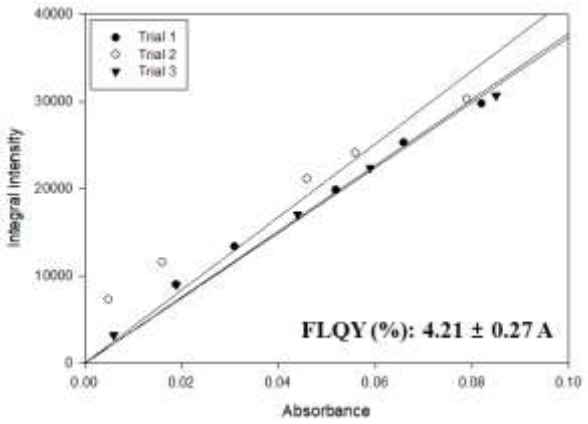
Trial 1
Trial 2
Trial 3
Integral intensity
Absorbance
FLQY (%): 4.21 ± 0.27 A

(C)

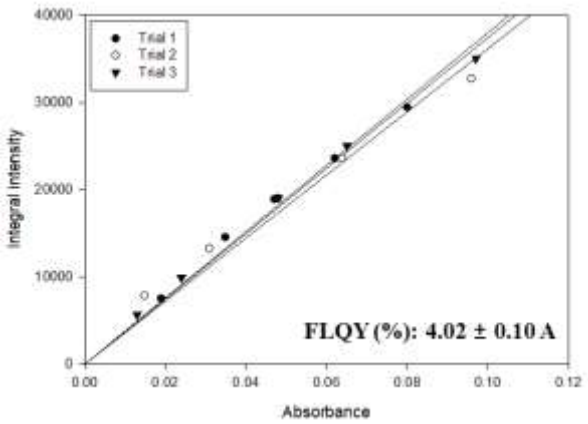
Trial 1
Trial 2
Trial 3
Integral intensity
Absorbance
FLQY (%): 4.02 ± 0.10 A

Fig 3 A linear plot of integral photoluminescence intensity (excitation: 360 nm; emission: 450 nm) for the absorption at 360 nm of carbon quantum dot (CQD) synthesized from spent coffee ground (SCG) at pH (A) 2.5, (B) 3.0, and (C) 4.0 obtained from three independent trials. Fluorescence quantum yield (FLQY) value was derived by comparing the derived slope with the reference value of quinine sulfate in 0.1 M H_2SO_4 (54 %). The same capital letter indicates no significant ($P > 0.05$) difference between values.

(A)

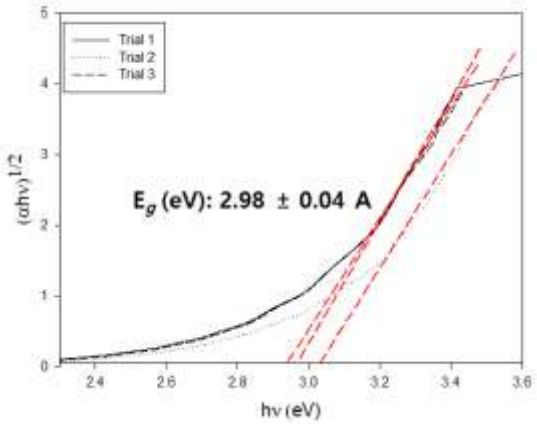
Trial 1
Trial 2
Trial 3
E_g (eV): 2.98 ± 0.04 A
$(\alpha h\nu)^{1/2}$
hν (eV)

(B)

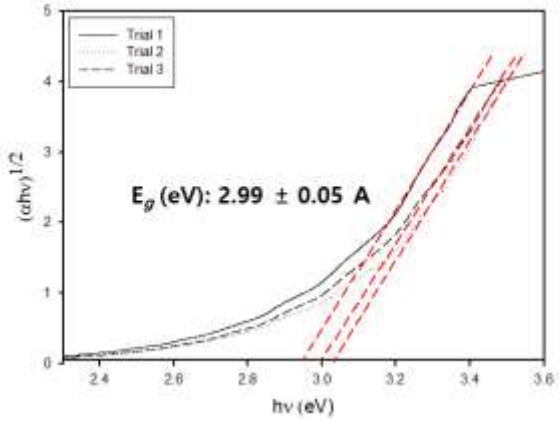
Trial 1
Trial 2
Trial 3
E_g (eV): 2.99 ± 0.05 A
$(\alpha h\nu)^{1/2}$
hν (eV)

(C)

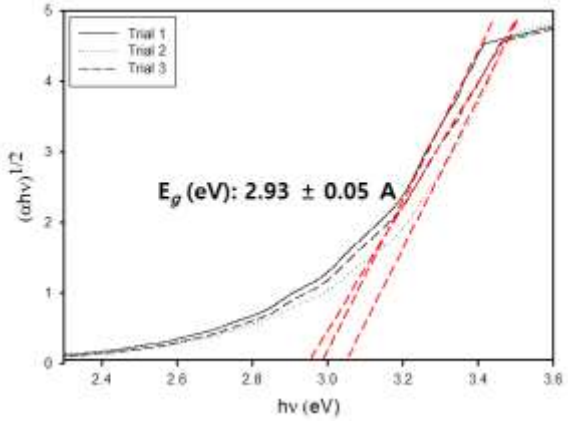
Trial 1
Trial 2
Trial 3
E_g (eV): 2.93 ± 0.05 A
$(\alpha h\nu)^{1/2}$
hν (eV)

Fig 4 Tauc plot of $(\alpha h\nu)^2$ for $h\nu$ of carbon quantum dot (CQD) synthesized from spent coffee ground (SCG) at pH (A) 2.5, (B) 3.0, and (C) 4.0 obtained from three independent trials. α, h, and ν are absorption coefficient, Planck constant, and light frequency, respectively. The band gap energy (E_g) was determined by calculating the intercept of the incident photon energy axis by adding the straight part of the plot. The same capital letter indicates no significant ($P > 0.05$) difference between values.

(A)

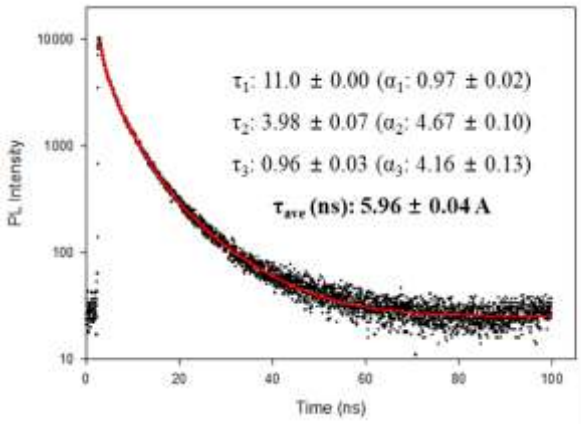
τ_1: 11.0 ± 0.00 (α_1: 0.97 ± 0.02)
τ_2: 3.98 ± 0.07 (α_2: 4.67 ± 0.10)
τ_3: 0.96 ± 0.03 (α_3: 4.16 ± 0.13)
τ_{ave} (ns): 5.96 ± 0.04 A
PL Intensity
Time (ns)

(B)

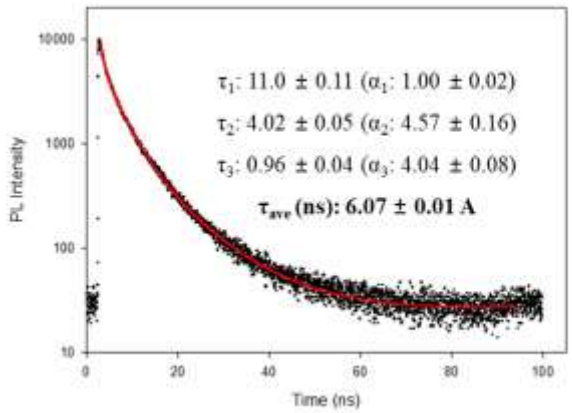
τ_1: 11.0 ± 0.11 (α_1: 1.00 ± 0.02)
τ_2: 4.02 ± 0.05 (α_2: 4.57 ± 0.16)
τ_3: 0.96 ± 0.04 (α_3: 4.04 ± 0.08)
τ_{ave} (ns): 6.07 ± 0.01 A
PL Intensity
Time (ns)

(C)

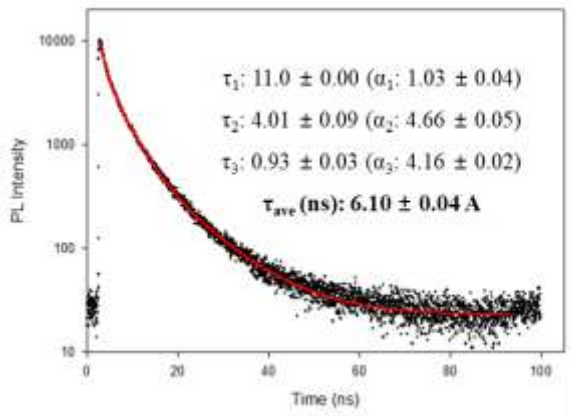
τ_1: 11.0 ± 0.00 (α_1: 1.03 ± 0.04)
τ_2: 4.01 ± 0.09 (α_2: 4.66 ± 0.05)
τ_3: 0.93 ± 0.03 (α_3: 4.16 ± 0.02)
τ_{ave} (ns): 6.10 ± 0.04 A
PL Intensity
Time (ns)

Fig 5 Time-resolved photoluminescence (PL) decay measurements of carbon quantum dot (CQD) synthesized from spent coffee ground (SCG) at pH (A) 2.5, (B) 3.0, and (C) 4.0 with excitation and emission wavelengths at 375 nm and 450 nm, respectively. Average fluorescence lifetime (τ_{ave}) was calculated using the following formula: $(a_1\tau_1^2 + a_2\tau_2^2 + a_3\tau_3^2)/(a_1\tau_1 + a_2\tau_2 + a_3\tau_3)$, where a_1, a_2, and a_3 are amplitudes as a normalized percentage (%) of the first, second, and third components, respectively, and τ_1, τ_2, and τ_3 are the PL lifetime (*ns*) of these components, respectively. The same capital letter indicates no significant ($P > 0.05$) difference between values.

3.4. Effect of zeta potential (mV) change of CQD and pathogens according to pH condition on uptake of CQD into cells

Interactions between bacteria and nanoparticles are driven by electrostatic or/and dispersive forces between functional groups on their surfaces (Hwang, Ahn, Mhin, & Kim, 2012). The surface charge of microorganisms is expressed by chemical functional groups on the cell surface such as -NH_2, -$CONH_2$, -COOH, -OH of lipopolysaccharide, lipoprotein, and surface proteins in the cell wall (C. Wang, Chang, Yang, & Cui, 2014). Almost all bacteria have a negative charge at neutral pH, it is known that cell surface charge can be changed by ionization of the surface functional group depending on environmental pH conditions (B. Li & Logan, 2004; C. Wang et al., 2014). It is also known that CQD has a surface charge determined by surface chemical functional groups such as COOH and NH_2 and that the charge can change according to protonation or deprotonation process of the functional group according to pH conditions (Wei et al., 2021). Therefore, it was hypothesized that the change in the surface charge of pathogens and CQD derived from SCG depending on pH conditions could induce a change in the interaction between them. Thus, zeta potentials were measured under each pH condition (pH 2.5, 3.0, and 4.0) (Fig. 6). At pH 4.0, zeta potentials of *E. coli* O157:H7 and CQD were -5.07, and -18.63 mV, respectively. When the pH decreased, their

negative zeta potentials also gradually decreased to -1.80, and -5.59 mV at pH 2.5, respectively. Several studies have shown that the degree of electrostatic attraction or repulsion between nanoparticles and bacteria changes when their surface charge (zeta potential) changes according to the pH condition. Accordingly, the degree of absorption of nanoparticles into bacteria also changes (Khan, Mukherjee, & Chandrasekaran, 2011; Khan, Srivatsan, Vaishnavi, Mukherjee, & Chandrasekaran, 2011; Neal, 2008). Therefore, it was hypothesized that when pH decreases, negative zeta potentials of CQD and bacteria also decrease along with the decrease of electrostatic repulsion, thereby getting closer between CQD and the pathogen and increasing interaction between them. To confirm the direct evidence of this hypothesis, the degree of uptake of CQD to pathogens according to pH conditions was measured. It was confirmed that as the pH decreased, the degree of CQD uptake to pathogens increased significantly ($P < 0.05$) (Fig. 7).

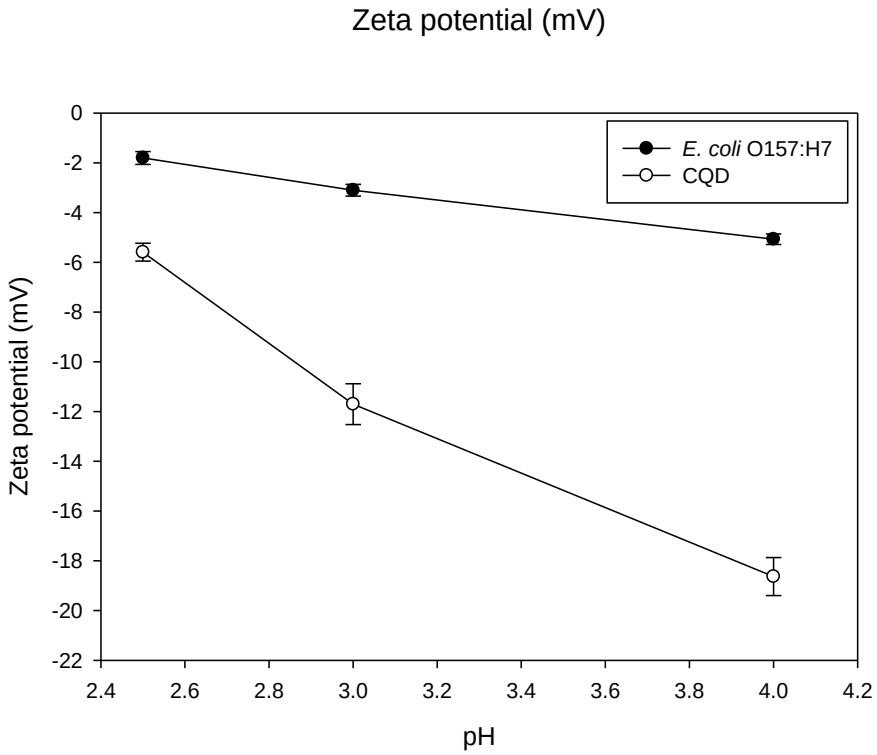

Fig 6 Zeta potentials (mV) of carbon quantum dot (CQD) synthesized from spent coffee ground (SCG) and *E. coli* O157:H7 at different pH condition (2.5, 3.0, and 4.0).

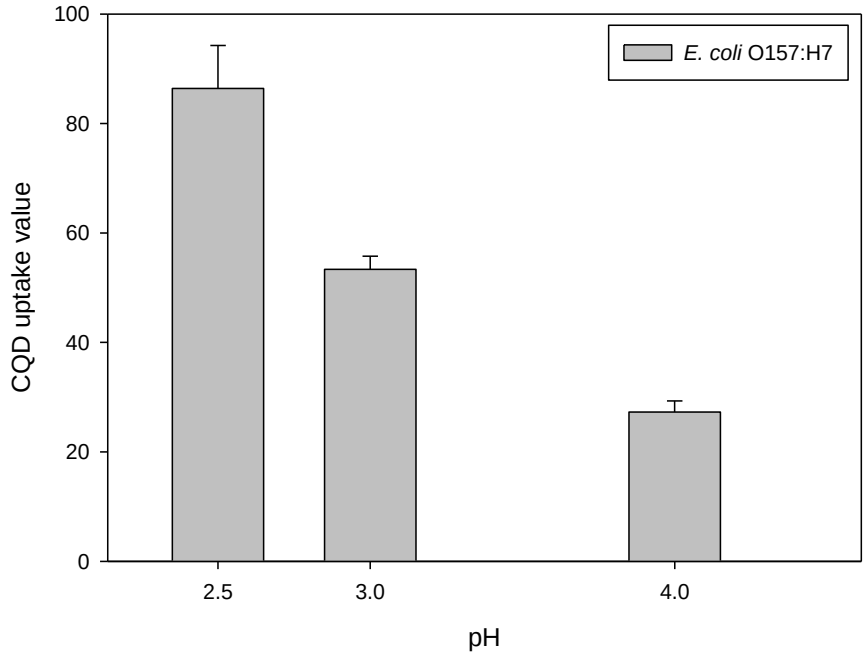

Fig 7 Uptake values of carbon quantum dot (CQD) synthesized from spent coffee ground (SCG) into cells of *E. coli* O157:H7 at different pH conditions (2.5, 3.5, and 4.0).

3.5. Investigation of ROS scavenger Changes within cells at different pH conditions

The VLD antimicrobial activity of CQD is mainly due to ROS it generates (J.-W. Kang et al., 2021). The ROS produced by VLD antimicrobial activity of CQD was investigated using ROS scavengers. Sodium pyruvate, mannitol, sodium azide, and trion were used as scavengers of H_2O_2, ·OH, $^1O_2$, and $O_2\cdot^-$, respectively (Franco, 2007; Liubimovskii, 2021). ROS that affected the antimicrobial activity by CQD was investigated with ROS scavengers. It was revealed that the degree of reduction levels (log CFU/mL) decreased significantly by adding sodium azide (Fig. 8). It was confirmed that singlet oxygen ($^1O_2$) served as the main bactericidal factor of *E. coli* O157:H7 in VLD antimicrobial activity of CQD. It is known that the lifetime of singlet oxygen is very short and disappears after a few nanoseconds (Skovsen& Esben, 2005). Even if the lifetime of $^1O_2$ lifetime is dependent on its environment such as solvent and temperature, the lifetime of $^1O_2$ short is within 55 ns, 12 μs, and 50.3 μs (Rodgers, 1983; Adams& Wilkinson, 1972; Peter& Ogilby, 1982). It can be seen that singlet oxygen disappears rapidly. Therefore, the distance between the bacteria and CQD in the aqueous solution is very important in order to inactivate pathogenic bacteria with ROS which was generated by CQD under visible light treatment. In a pH 2.5 aqueous solution, a relatively

close distance between CQD and pathogen due to decreased negative zeta potential made it possible for $^1O_2$ to inactivate *E. coli* O157:H7. As the pH increases, the distance between CQD and bacteria increases due to the increase of the negative zeta potential, and the inactivation of bacteria by $^1O_2$ decreases (Fig. 8B, 8C).

(A)

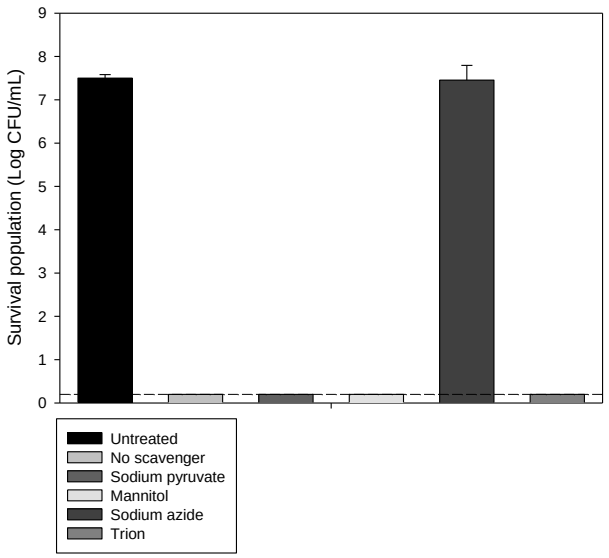
Survival population (Log CFU/mL)
0
1
2
3
4
5
6
7
8
9
Untreated
No scavenger
Sodium pyruvate
Mannitol
Sodium azide
Trion

(B)

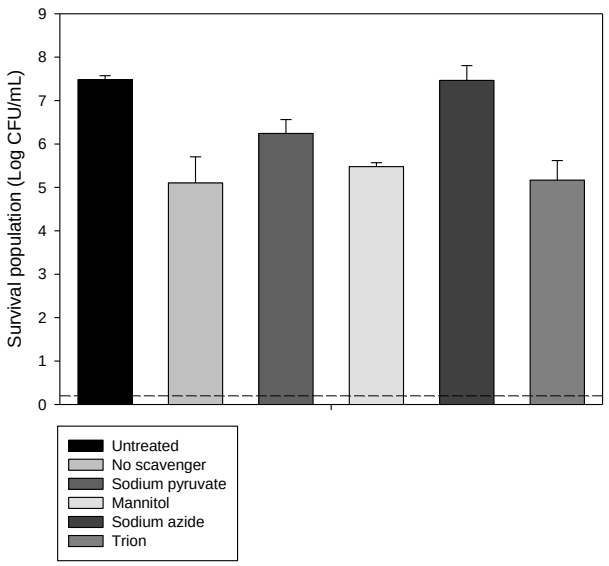
Survival population (Log CFU/mL)
0
1
2
3
4
5
6
7
8
9
Untreated
No scavenger
Sodium pyruvate
Mannitol
Sodium azide
Trion

(C)

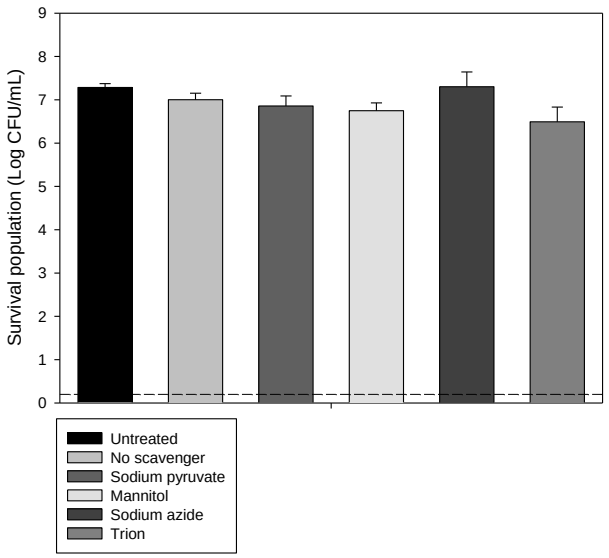

Fig 8 Survival population of *E. coli* O157:H7 in PBS after CQD treatment (1 mg/mL) with visible light (28.8 J/cm^2) at pH (A) 2.5, (B) 3.0, and (C) 4.0. Sodium pyruvate, mannitol, sodium azide, and trion were used as ROS scavengers. Limitation of detection was detection limit was 1.00 Log CFU/mL.

3.6. Changes in activities of ROS defense enzymes within cells at different pH conditions

Living organisms can generate ROS as by-products of aerobic metabolism. They can protect themselves from the risk of oxidative damage caused by ROS using several defense systems that can scavenge ROS (Yao, Min, & Lv, 2006). Catalase (CAT) and superoxide dismutase (SOD) are the most well-known enzymes in the ROS defense system of cells (L. Li et al., 2007). As extracellular pH changes, the intracellular pH also changes in a positive correlation due to pH gradient (Campolongo, Siegumfeldt, Aabo, Cocolin, & Arneborg, 2014; Hansen, Johansen, Marten, Wilmes, Jespersen, & Arneborg, 2016). ROS defense enzymes have a characteristic that their activity decreases as pH decreases from a neutral pH (Alptekin, Tükel, & Yildirim, 2008; Danial & Alkhalaf, 2020). Based on this fact, it was hypothesized that the activities of ROS defense enzymes would change with changing internal pH of pathogens when pH conditions were changed. Thus, the activities of CAT and SOD as representative ROS defense enzymes were measured under each pH condition (pH 2.5, 3.0, and 4.0). As expected, activities of ROS defense enzymes (SOD and CAT) of *E. coli* O157:H7 decreased significantly ($P < 0.05$) as the pH decreased (Fig. 9). It is considered that the activity gradually decreases due to changes in three-dimensional

structures of enzymes according to a decrease of the pH inside cells (Scopes, 2001).

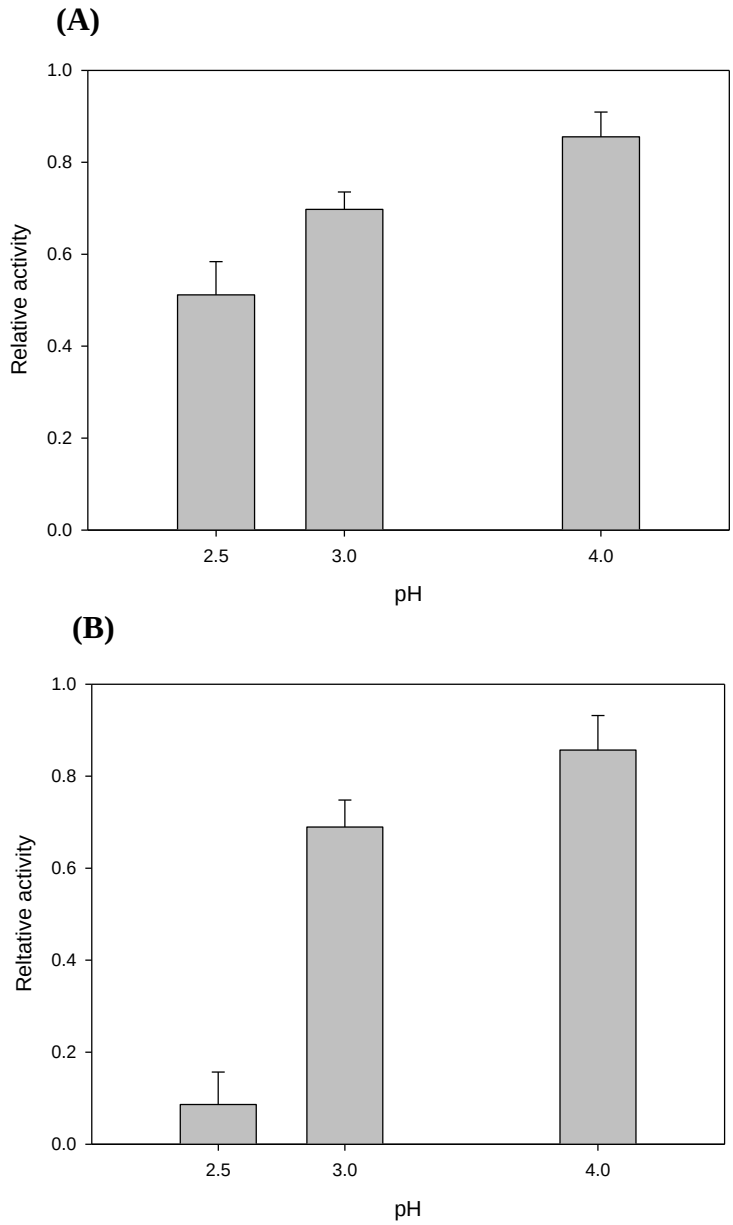

Fig 9 Relative activity of (A) superoxide dismutase (SOD) and (B) catalase (CAT) of *E. coli* O157:H7 at different pH conditions (2.5, 3.0, and 4.0). Relative activity of SOD and CAT at pH 7 was set to 1.

3.7. Changes in the degree of intracellular ROS (iROS) generation and oxidative damage at different pH conditions

Combining the results of Fig. 6, 7, 8 and 9, it could be interpreted that as pH decreases, the electrostatic repulsion between CQD and pathogen also decreases, resulting in enhanced interaction between CQD and pathogens. At the same time, the ROS scavenging activity decreases. Thus, the amount of ROS remaining without being scavenged increases in addition to the occurrence of more ROS inside cells, resulting in increased cell damage caused by ROS, which eventually leads to an increase in VLD antimicrobial activity of CQD. In order to prove this interpretation, the amount of ROS generated inside cells caused by CQD was examined at each pH condition (pH 2.5, 3.0, and 4.0) under visible light treatment. To measure the amount of ROS accumulated in cells, iROS generation values were measured using H_2DCFDA that could permeate into cells and become oxidized by iROS to 2',7'-dichlorofluorescein (DCF) known to emit fluorescence. Thus, the amount of iROS generation can be measured through the degree of DCF generation (Yoon, Lee, & Cha, 2018). After treatment with 28.8 J/cm^2 of visible light, iROS was not generated at pH 4.0 regardless of the presence or absence of CQD. However, iROS was generated at pH 3.0 and 2.5 in the presence of CQD, showing significantly ($P < 0.05$) higher values at pH 2.5 (Fig. 10). To examine

whether the increased amount of iROS actually induced more cellular damage, damage to the cell membrane that could lead to death by reducing the ability of microorganisms to maintain homeostasis for life activities was measured representatively among various cell components (Park & Kang, 2013). The degree of cell membrane damage was measured using PI that could not penetrate an intact membrane, but could emit fluorescence by penetrating the cell membrane with physical destruction (Hewitt & Nebe-Von-Caron, 2004). As shown in Fig. 11A, when 28.8 J/cm^2 of visible light was used for treatment in the presence of CQD, cell membrane damage did not appear at pH 4.0, whereas damage was observed at pH 2.5 and 3.0, showing significantly ($P <$ 0.05) larger value at pH 2.5, consistent with results of iROS generation and antimicrobial effect. Finally, to prove the direct correlation between the amount of iROS generation and cell membrane damage, it was necessary to confirm that the cell membrane damage was caused by ROS. Fatty acid, one of the essential cellular materials, is mainly present in the cell membrane in the form of acyl phospholipid. The more peroxidation of lipids in the cell membrane occurs, the more permeability of cell will occur, which may cause cell membrane damage. (Gutteridge, 1995; Kaneda, 1991). Therefore, the degree of lipid peroxidation in the cell membrane was measured using Tbars. Lipid peroxides are known to be unstable that produces reactive compounds,

such as malondialdehyde (MDA) and 4-hydroxynonenal(4-HNE)(Dix & Aikens, 1993). MDA easily reacts with TBA forming MDA-TBA adduct and its concentration can be detected fluorometrically(Fernández, Pérez-Álvarez, & Fernández-López, 1997). As shown in Fig. 11B, the occurrence of lipid peroxidation in the cell membrane showed a trend consistent with the result of cell membrane damage.

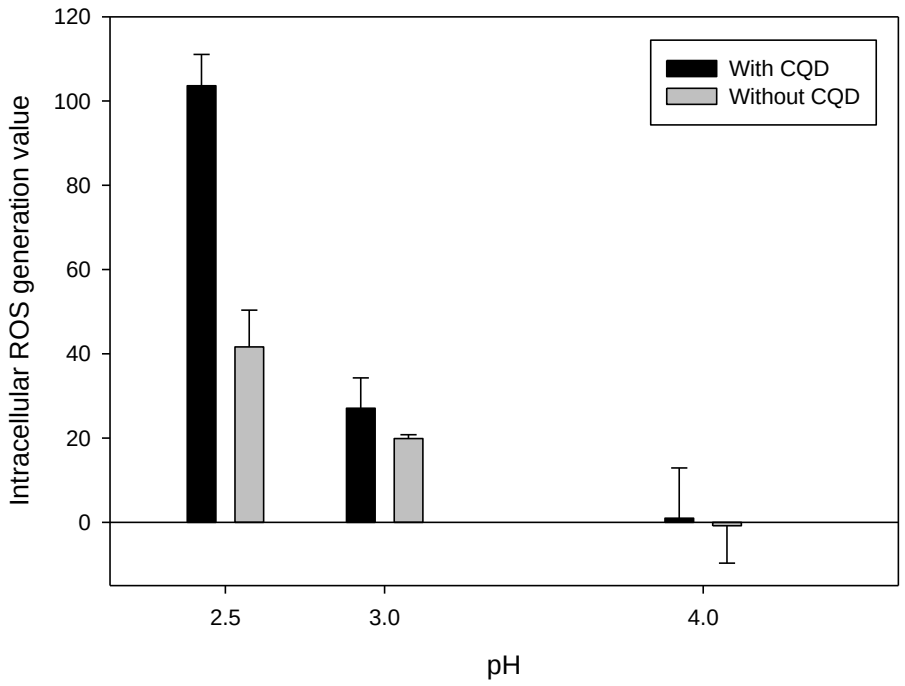

Fig 10 Intracellular reactive oxygen species (iROS) generation of *E. coli* O157:H7 in PBS with or without 1 mg/mL of carbon quantum dot (CQD) synthesized from spent coffee ground (SCG) at different pH conditions (2.5, 3.0, and 4.0) under visible light treatment of 28.8 J/cm^2. The error bars indicate standard deviations.

(A)

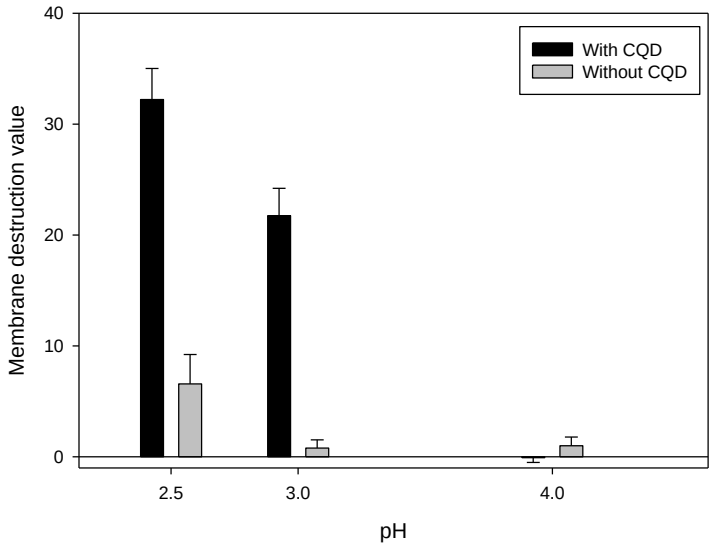
40
30
20
10
0
Membrane destruction value
With CQD
Without CQD
2.5
3.0
4.0
pH

(B)

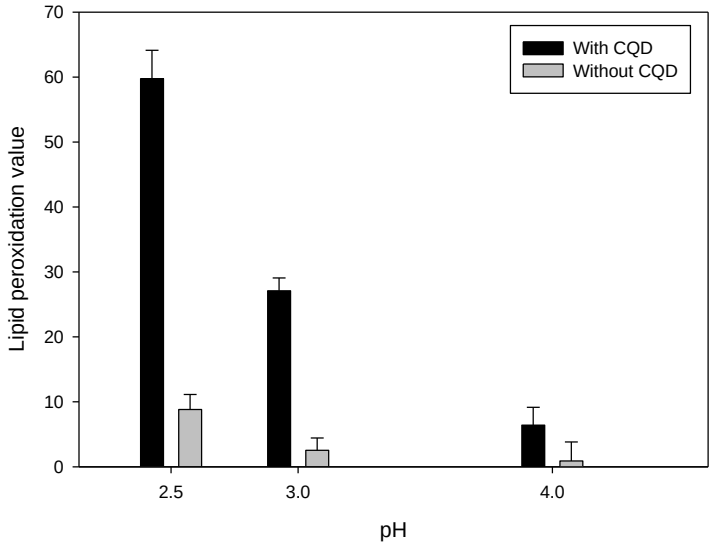
70
60
50
40
30
20
10
0
Lipid peroxidation value
With CQD
Without CQD
2.5
3.0
4.0
pH

Fig 11 Membrane damage values obtained by measuring (A) Propidium Iodide (PI) uptake values and (B) Thiobarbituric Acid Assay (Tbars) value of *E. coli* O157:H7 in PBS with or without 1 mg/mL of carbon quantum dot (CQD) synthesized from spent coffee ground (SCG) at different pH conditions (2.5, 3.0, and 4.0) under visible light treatment of 28.8 J/cm^2. The error bars indicate standard deviations.

3.8. Application in washing process with VLD antimicrobial activities of CQD

To investigate whether CQD concentration affects the degree of inactivation or not, 1, 3, and 5 mg/mL CQD concentration solutions were prepared and VDL inactivation was applied. Fig. 12 shows the survival populations of bacteria on the surface of apples after treatment with different CQD concentrations. Because pH was set to 2.5, inactivation occurred even in dark conditions. Nevertheless, in the presence of visible light, for both inoculated and uninoculated samples, a significantly greater inactivation was observed compared to dark for each dose and CQD concentration. Nevertheless, Fig. 12A shows that there is still 3.21 Log CFU/sample after treatment of 115.2 J/cm^2 at a CQD concentration of 1 mg/mL under visible light on the inoculated sample. Similarly, Table 2 shows, still 2.67 Log CFU/ 20 mL remained in wash water after 115.2 J/cm^2 treatment at a CQD concentration of 1 mg/mL under visible light. It means more effective treatment conditions have to be established to prevent cross-contamination. However, when CQD concentration was increased to 3 and 5 mg/mL, counts of *E. coli* O157:H7 both on the inoculated and uninoculated sample were reduced to below the detection limit (detection limit = 1.70 Log CFU/sample) after treatment of 115.2 J/cm^2 (Fig. 12B, 12C). In addition, pathogen was

inactivated to the detection limit on wash water after treatment of 115.2 J/cm^2 (detection limit = 1.30 Log CFU/ 20 mL) (Table 2).

To sum up, CQD solution (CQD concentration of 3 and 5 mg/mL) with visible light are able to inactivate *E. coli* O157:H7 to the detection limit, not only in solid but also in liquid. Therefore, in subsequent experiments, 3 mg/mL was selected for optimal CQD concentration for VLD inactivation and fixed for further experiments.

(A)

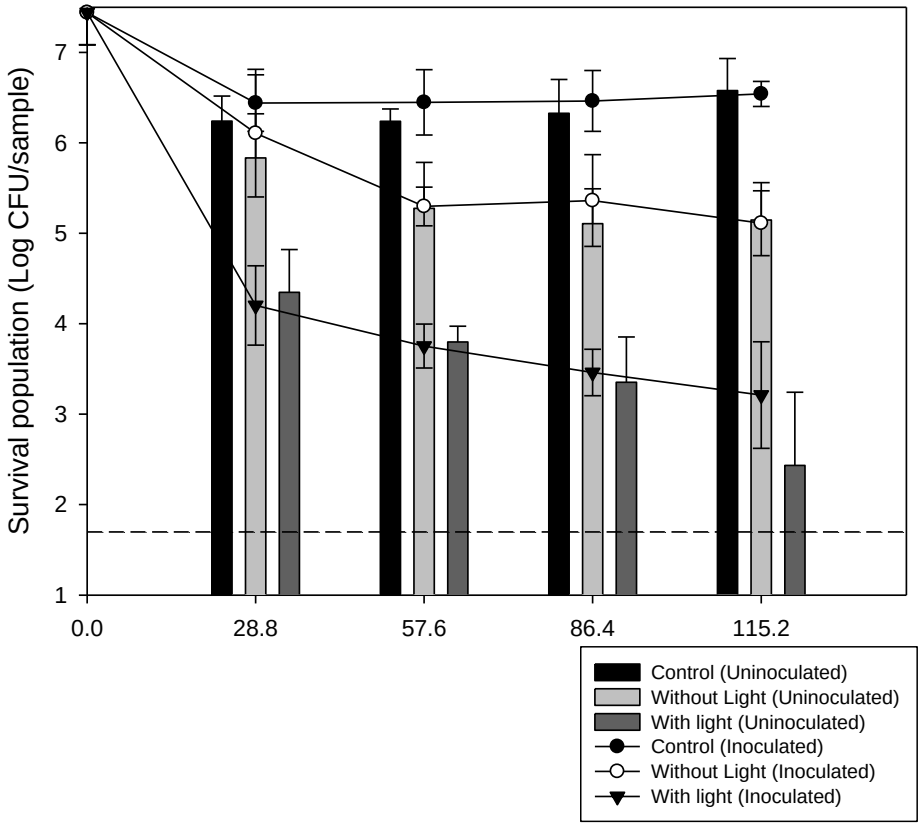
Survival population (Log CFU/sample)
7
6
5
4
3
2
1
0.0
28.8
57.6
86.4
115.2
Control (Uninoculated)
Without Light (Uninoculated)
With light (Uninoculated)
Control (Inoculated)
Without Light (Inoculated)
With light (Inoculated)

(B)

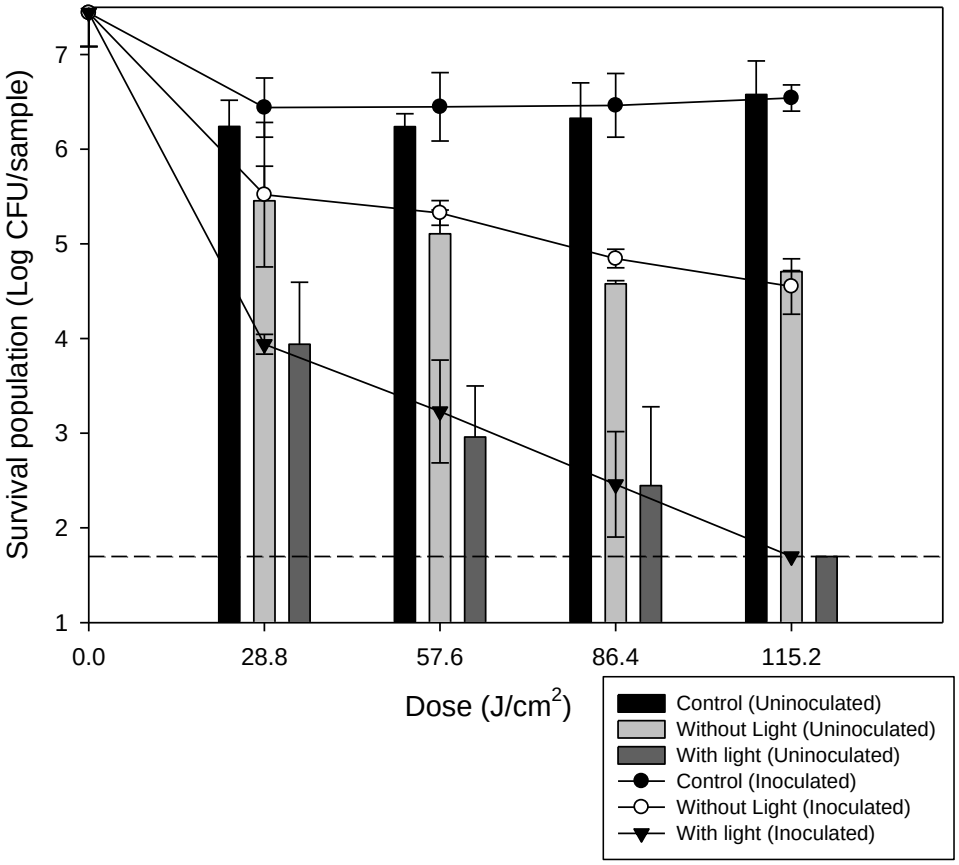
Survival population (Log CFU/sample)
7
6
5
4
3
2
1
0.0
28.8
57.6
86.4
115.2
Dose (J/cm2)
Control (Uninoculated)
Without Light (Uninoculated)
With light (Uninoculated)
Control (Inoculated)
Without Light (Inoculated)
With light (Inoculated)

(C)

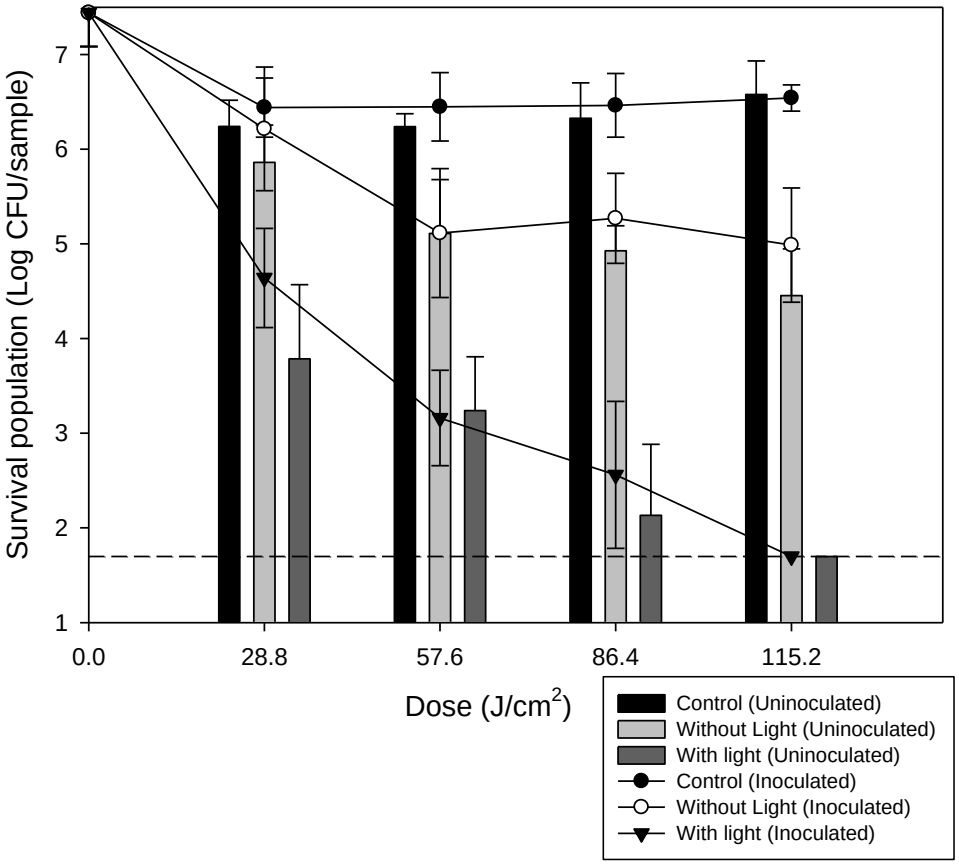

Fig 12 Survival population (Log CFU/sample) of *E. coli* O157: H7 on apple slices with CQD concentration of (A) 1 mg/mL, (B) 3 mg/mL, and (C) 5 mg/mL under visible light or dark treatment. The error bars indicate standard deviations. Limitation of detection was 1.70 Log CFU/sample.

Table 2 Survival population (Log CFU/20 mL) of *E. coli* O157:H7 enumerated from liquid (20 mL) after washing with simulated cross-contamination with CQD concentration of (A) 1 mg/mL, (B) 3 mg/mL, and (C) 5 mg/mL

(A)

	Survival population (Log CFU/20 mL)			
Dose (J/cm^2)	28.8	57.6	86.4	115.2
Control	8.52 ±0.28 Aa	8.51 ±0.34 Aa	8.56 ±0.34 Aa	8.59 ±0.43 Aa
Dark	6.26 ±0.61Ab	5.36 ±0.61 ABb	5.02 ±0.72 ABb	5.15 ±0.51 Bb
Light	4.22 ±0.17 Ac	3.41 ±0.20 Bc	3.25 ±0.16 Bc	2.67 ±0.21 Cc

(B)

	Survival population (Log CFU/20 mL)			
Dose (J/cm^2)	28.8	57.6	86.4	115.2
Control	8.52 ±0.28 Aa	8.34 ±0.38 Aa	8.16 ±0.38 Aa	8.04 ±0.40 Aa
Dark	6.29 ±0.58Ab	5.00 ±0.16 Bb	4.80 ±0.25 Bb	4.73 ±0.41 Bb
Light	4.05 ±0.13 Ac	1.86 ±0.54 Bc	1.84 ±0.50 Bc	N.D

(C)

Dose (J/cm^2)	Survival population (Log CFU/20 mL)			
	28.8	57.6	86.4	115.2
Control	8.46 ±0.07 Aa	8.34 ±0.38 Aa	8.16 ±0.38 Aa	8.04 ±0.40 Aa
Dark	7.10 ±0.78 Ab	5.29 ±0.64 Bb	4.71 ±0.67 Bb	4.51 ±0.37 Bb
Light	3.49 ±0.31 Ac	1.66 ±0.62 Bc	N.D	N.D

The error bars indicate standard deviations. Means with the different capital letters within the same row are significantly different ($P < 0.05$). Means with different lowercase letters within the same column are significantly different ($P < 0.05$). Limitation of detection was 1.30 Log CFU/20 mL.
N.D= Not detected.

3. 9. Evaluation of reusability and activity change over time of CQD

To evaluate reusability of CQD, solution of CQD was reused in the next treatment. Fig. 13 shows the bacterial population of *E. coli* O157:H7 enumerated from three consecutive cycles of VLD inactivation of CQD. Even after reuse, more than 5 Log CFU/sample reduction occurred after 86.4 J/cm^2 treatment for each treatment. And counts of *E. coli* O157:H7 on inoculated sample were inactivated to below the detection limit (detection limit = 1.70 Log CFU/sample) after 115.2 J/cm^2 treatment for each treatment (Data not shown). This result means CQD can be reused for VLD antimicrobial inactivation for at least three cycles. In case of chlorine, when chlorine reacts with dissolved organic matter from fresh produce, sanitation efficacy may reduce (Shen, Luo, Nou, Wang, & Millner, 2013). If sanitizing agents can't be reused, it may not only be economically detrimental, but may also lead to severe wastage of water. In this respect, CQD can be used as an economical sanitizing agent because it is reusable. Fig. 14 indicates the degree of inactivation depending on the storage time of CQD for 4 weeks. For CQD stored at 4°C, inactivation more than 4 log CFU/sample occurred on the first day of CQD synthesis and there was no significant ($P > 0.05$) difference in VLD inactivation from the first day to the 4th week. This means that synthesized CQD can be applied to VLD inactivation for at least 4 weeks.

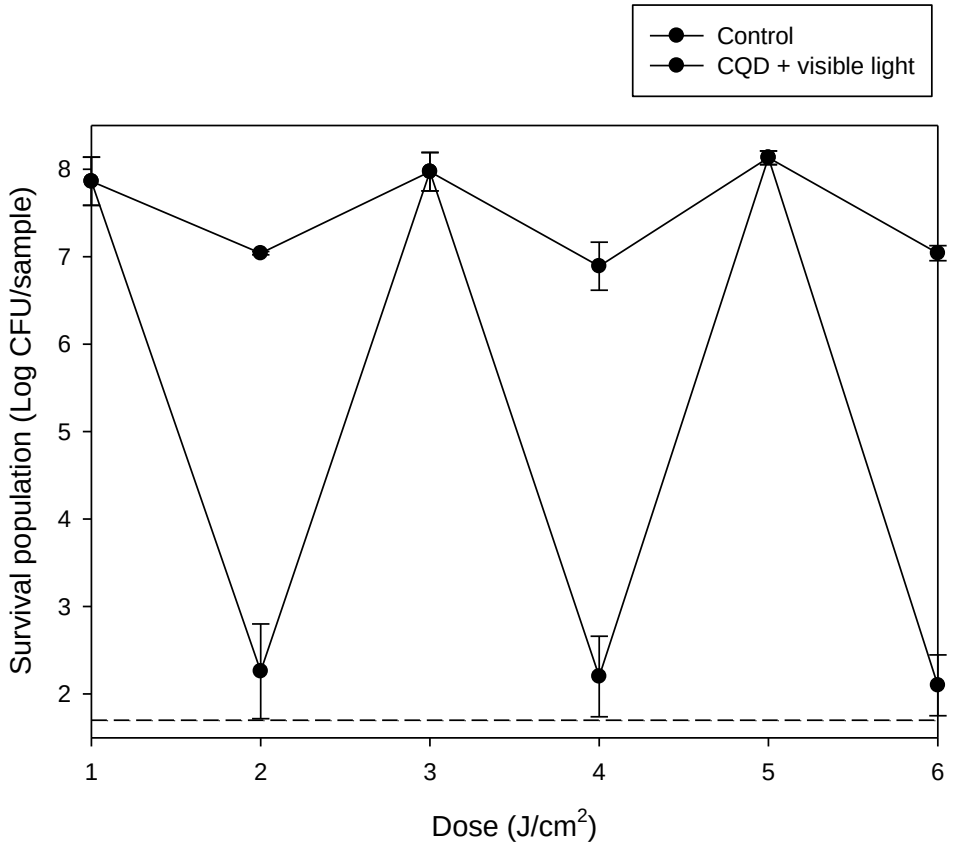

Fig 13 Bacterial population (Log CFU/sample) of *E. coli* O157:H7 from three consecutive cycles of CQD (3 mg/mL) + visible light of 86.4 J/cm^2 treatment. The error bars indicate standard deviations. Limitation of detection was 1.70 Log CFU/sample.

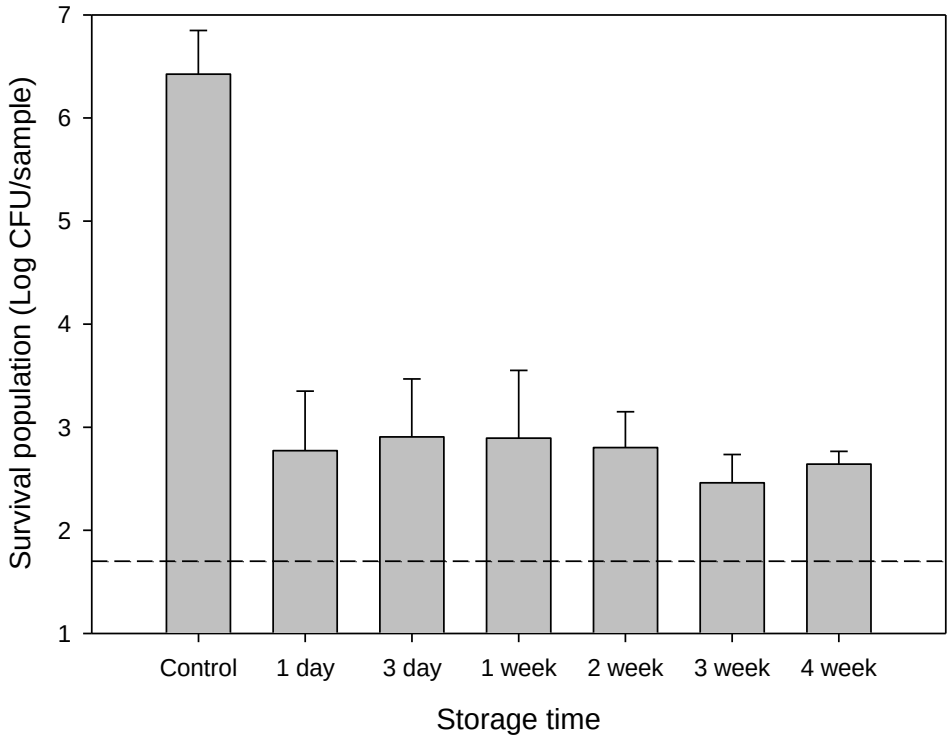

Fig 14 Bacterial population (Log CFU/sample) of *E. coli* O157:H7 from different storage period of CQD (3 mg/mL) + visible light of 86.4 J/cm^2 treatment. Storage temperature at 4°C. The error bars indicate standard deviations. Limitation of detection was 1.70 Log CFU/sample.

IV. CONCLUSION

In this study, CQD showing VLD antimicrobial activity as a high value-added material was successfully synthesized using SCG as biomass. CQD synthesized from SCG showed improved VLD antimicrobial activity under acidic condition. Various analyses demonstrated that the decrease in repulsion between pathogenic bacteria and CQD and decrease in ROS defense enzyme activity in the cell were causes for the improvement of the VLD antimicrobial activity according to a decrease in pH. This means that in order to effectively utilize CQD synthesized from SCG, it is advantageous to use it under acidic conditions. Thus, CQD is expected to be more effective when it is applied in combination with substances such as organic acid. Furthermore, CQD can be used as sanitizing agents under visible light. Especially, VLD antimicrobial activity with CQD can be applied to fresh produce washing process. CQD solution is cost-effective as it can be reused and it can remain its activity during storage. This study can be as baseline data for synthesizing CQD from biomass and applying for photodynamic inactivation. Further research is needed to develop a synthetic method that can change surface characteristics so that it can show antimicrobial activity even at neutral and alkaline pH for wider applications.

V. REFERENCES

Abd Rani, U., Ng, L. Y., Ng, C. Y., & Mahmoudi, E. (2020). A review of carbon quantum dots and their applications in wastewater treatment. *Advances in Colloid and Interface Science, 278*, 102124.

Adams, D. R., & Wilkinson, F. (1972). Lifetime of singlet oxygen in liquid solution. Journal of the Chemical Society, Faraday Transactions 2: Molecular and Chemical Physics, 68, 586-593.

Al Awak, M. M., Wang, P., Wang, S., Tang, Y., Sun, Y.-P., & Yang, L. (2017). Correlation of carbon dots' light-activated antimicrobial activities and fluorescence quantum yield. *RSC advances, 7*(48), 30177-30184.

Alam, A.-M., Park, B.-Y., Ghouri, Z. K., Park, M., & Kim, H.-Y. (2015). Synthesis of carbon quantum dots from cabbage with down-and up-conversion photoluminescence properties: excellent imaging agent for biomedical applications. *Green Chemistry, 17*(7), 3791-3797.

Alptekin, Ö., Tükel, S. S., & Yildirim, D. (2008). Immobilization and characterization of bovine liver catalase on eggshell. *Journal of the Serbian Chemical Society, 73*(6), 609-618.

Ameen, A. P., Ward, R., Short, R., Beamson, G., & Briggs, D. (1993). A high-resolution X-ray photoelectron spectroscopy study of trifluoroacetic

anhydride labelling of hydroxyl groups: demonstration of the β shift due to OC (O) CF3. *Polymer*, *34*(9), 1795-1799.

Ando, Y., & Akiyama, H. (2010). pH-dependent fluorescence spectra, lifetimes, and quantum yields of firefly-luciferin aqueous solutions studied by selective-excitation fluorescence spectroscopy. *Japanese journal of applied physics*, *49*(11R), 117002.

Babbar, N., & Oberoi, H. S. (2014). Enzymes in value-addition of agricultural and agro-industrial residues. *Enzymes in value-addition of wastes*, 29-50.

Bandi, R., Gangapuram, B. R., Dadigala, R., Eslavath, R., Singh, S. S., & Guttena, V. (2016). Facile and green synthesis of fluorescent carbon dots from onion waste and their potential applications as sensor and multicolour imaging agents. *RSC advances*, *6*(34), 28633-28639.

Campolongo, S., Siegumfeldt, H., Aabo, T., Cocolin, L., & Arneborg, N. (2014). The effects of extracellular pH and hydroxycinnamic acids influence the intracellular pH of Brettanomyces bruxellensis DSM 7001. *LWT-Food Science and Technology*, *59*(2), 1088-1092.

Campos-Vega, R., Loarca-Pina, G., Vergara-Castañeda, H. A., & Oomah, B. D. (2015). Spent coffee grounds: A review on current research and future prospects. *Trends in Food Science & Technology*, *45*(1), 24-36.

Casal, S., Mendes, E., Oliveira, M., & Ferreira, M. (2005). Roast effects on coffee amino acid enantiomers. *Food chemistry, 89*(3), 333-340.

Chen, C., Su, H., Lu, L.-N., Hong, Y.-S., Chen, Y., Xiao, K., . . . Liu, Z.-Q. (2021). Interfacing spinel NiCo2O4 and NiCo alloy derived N-doped carbon nanotubes for enhanced oxygen electrocatalysis. *Chemical Engineering Journal, 408*, 127814.

Cruz, R., Cardoso, M. M., Fernandes, L., Oliveira, M., Mendes, E., Baptista, P., . . . Casal, S. (2012). Espresso coffee residues: a valuable source of unextracted compounds. *Journal of agricultural and food chemistry, 60*(32), 7777-7784.

Danial, E. N., & Alkhalaf, M. I. (2020). Co-immobilisation of superoxide dismutase and catalase using an in vitro encapsulation protocol. *Journal of King Saud University-Science, 32*(4), 2489-2494.

Ding, Q., & Tikekar, R. V. (2020). The synergistic antimicrobial effect of a simultaneous UV-A light and propyl paraben (4-hydroxybenzoic acid propyl ester) treatment and its application in washing spinach leaves. *Journal of food process engineering, 43*(1), e13062.

Dong, X., Bond, A. E., Pan, N., Coleman, M., Tang, Y., Sun, Y.-P., & Yang, L. (2018). Synergistic photoactivated antimicrobial effects of carbon

dots combined with dye photosensitizers. *International Journal of Nanomedicine*, *13*, 8025.

Dong, X., Liang, W., Meziani, M. J., Sun, Y.-P., & Yang, L. (2020). Carbon dots as potent antimicrobial agents. *Theranostics*, *10*(2), 671.

Dong, X., Overton, C. M., Tang, Y., Darby, J. P., Sun, Y.-P., & Yang, L. (2021). Visible Light-Activated Carbon Dots for Inhibiting Biofilm Formation and Inactivating Biofilm-Associated Bacterial Cells. *Frontiers in bioengineering and biotechnology*, 1066.

Ebikade, E. O., Sadula, S., Gupta, Y., & Vlachos, D. G. (2021). A review of thermal and thermocatalytic valorization of food waste. *Green Chemistry*, *23*(8), 2806-2833.

Franco, R., Panayiotidis, M. I., & Cidlowski, J. A. (2007). Glutathione depletion is necessary for apoptosis in lymphoid cells independent of reactive oxygen species formation. Journal of biological chemistry, 282(42), 30452-30465.

Gardner, C. D., Hartle, J. C., Garrett, R. D., Offringa, L. C., & Wasserman, A. S. (2019). Maximizing the intersection of human health and the health of the environment with regard to the amount and type of protein produced and consumed in the United States. *Nutrition reviews*, *77*(4), 197-215.

Grabolle, M., Spieles, M., Lesnyak, V., Gaponik, N., Eychmüller, A., & Resch-Genger, U. (2009). Determination of the fluorescence quantum yield of quantum dots: suitable procedures and achievable uncertainties. *Analytical chemistry, 81*(15), 6285-6294.

Gutteridge, J. (1995). Lipid peroxidation and antioxidants as biomarkers of tissue damage. *Clinical chemistry, 41*(12), 1819-1828.

Hansen, G., Johansen, C. L., Marten, G., Wilmes, J., Jespersen, L., & Arneborg, N. (2016). Influence of extracellular pH on growth, viability, cell size, acidification activity, and intracellular pH of Lactococcus lactis in batch fermentations. *Applied microbiology and biotechnology, 100*(13), 5965-5976.

Hewitt, C. J., & Nebe-Von-Caron, G. (2004). The application of multi-parameter flow cytometry to monitor individual microbial cell physiological state. *Physiological stress responses in bioprocesses*, 197-223.

Hwang, G., Ahn, I.-S., Mhin, B. J., & Kim, J.-Y. (2012). Adhesion of nano-sized particles to the surface of bacteria: mechanistic study with the extended DLVO theory. *Colloids and Surfaces B: Biointerfaces, 97*, 138-144.

Jansen, R., & Van Bekkum, H. (1995). XPS of nitrogen-containing functional groups on activated carbon. *Carbon, 33*(8), 1021-1027.

Kaneda, T. (1991). Iso-and anteiso-fatty acids in bacteria: biosynthesis, function, and taxonomic significance. *Microbiological reviews, 55*(2), 288-302.

Kang, C., Huang, Y., Yang, H., Yan, X. F., & Chen, Z. P. (2020). A review of carbon dots produced from biomass wastes. *Nanomaterials, 10*(11), 2316.

Kang, J.-W., & Kang, D.-H. (2021). Effect of amino acid-derived nitrogen and/or sulfur doping on the visible-light-driven antimicrobial activity of carbon quantum dots: A comparative study. *Chemical Engineering Journal, 420,* 129990.

Kavaklı, P. A., Kavaklı, C., Seko, N., Tamada, M., & Güven, O. (2016). Radiation induced emulsion graft polymerization of 4-vinylpyridine onto PE/PP nonwoven fabric for As (V) adsorption. *Radiation Physics and Chemistry, 127,* 13-20.

Khan, S. S., Mukherjee, A., & Chandrasekaran, N. (2011). Studies on interaction of colloidal silver nanoparticles (SNPs) with five different bacterial species. *Colloids and Surfaces B: Biointerfaces, 87*(1), 129-138.

Khan, S. S., Srivatsan, P., Vaishnavi, N., Mukherjee, A., & Chandrasekaran, N. (2011). Interaction of silver nanoparticles (SNPs) with bacterial extracellular proteins (ECPs) and its adsorption isotherms and kinetics. *Journal of hazardous materials, 192*(1), 299-306.

Kou, X., Jiang, S., Park, S.-J., & Meng, L.-Y. (2020). A review: recent advances in preparations and applications of heteroatom-doped carbon quantum dots. *Dalton Transactions, 49*(21), 6915-6938.

Lei, C.-W., Hsieh, M.-L., & Liu, W.-R. (2019). A facile approach to synthesize carbon quantum dots with pH-dependent properties. *Dyes and Pigments, 169*, 73-80.

Li, B., & Logan, B. E. (2004). Bacterial adhesion to glass and metal-oxide surfaces. *Colloids and Surfaces B: Biointerfaces*, *36*(2), 81-90.

Li, L., Ng, T., Song, M., Yuan, F., Liu, Z., Wang, C., . . . Liu, F. (2007). A polysaccharide–peptide complex from abalone mushroom (Pleurotus abalonus) fruiting bodies increases activities and gene expression of antioxidant enzymes and reduces lipid peroxidation in senescence-accelerated mice. *Applied microbiology and biotechnology, 75*(4), 863-869.

Li, P., Yang, X., Zhang, X., Pan, J., Tang, W., Cao, W., . . . Xing, X. (2020). Surface chemistry-dependent antibacterial and antibiofilm activities of

polyamine-functionalized carbon quantum dots. *Journal of Materials Science, 55*(35), 16744-16757.

Li, Y., Liu, D., Zhu, C., Shen, X., Liu, Y., & You, T. (2020). Sensitivity programmable ratiometric electrochemical aptasensor based on signal engineering for the detection of aflatoxin B1 in peanut. *Journal of hazardous materials, 387*, 122001.

Liubimovskii, S. O., Ustynyuk, L. Y., & Tikhonov, A. N. (2021). Superoxide radical scavenging by sodium 4, 5-dihydroxybenzene-1, 3-disulfonate dissolved in water: Experimental and quantum chemical studies. Journal of Molecular Liquids, 333, 115810.

Liu, Y.-R., Shang, X., Gao, W.-K., Dong, B., Li, X., Li, X.-H., . . . Liu, C.-G. (2017). In situ sulfurized CoMoS/CoMoO 4 shell–core nanorods supported on N-doped reduced graphene oxide (NRGO) as efficient electrocatalyst for hydrogen evolution reaction. *Journal of Materials Chemistry A, 5*(6), 2885-2896.

Liu, Y., Zhou, L., Li, Y., Deng, R., & Zhang, H. (2017). Highly fluorescent nitrogen-doped carbon dots with excellent thermal and photo stability applied as invisible ink for loading important information and anti-counterfeiting. *Nanoscale, 9*(2), 491-496.

Lu, F., Zhou, Y.-h., Wu, L.-h., Qian, J., Cao, S., Deng, Y.-f., & Chen, Y. (2019). Highly fluorescent nitrogen-doped graphene quantum dots' synthesis and their applications as Fe (III) ions sensor. *International Journal of Optics, 2019*.

Martinez-Saez, N., García, A. T., Pérez, I. D., Rebollo-Hernanz, M., Mesías, M., Morales, F. J., . . . Del Castillo, M. D. (2017). Use of spent coffee grounds as food ingredient in bakery products. *Food chemistry, 216*, 114-122.

Meierhofer, F., Dissinger, F., Weigert, F., Jungclaus, J. r., Müller-Caspary, K., Waldvogel, S. R., . . . Voss, T. (2020). Citric acid based carbon dots with amine type stabilizers: pH-specific luminescence and quantum yield characteristics. *The Journal of Physical Chemistry C, 124*(16), 8894-8904.

Meng, W., Bai, X., Wang, B., Liu, Z., Lu, S., & Yang, B. (2019). Biomass-derived carbon dots and their applications. *Energy & Environmental Materials, 2*(3), 172-192.

Meziani, M. J., Dong, X., Zhu, L., Jones, L. P., LeCroy, G. E., Yang, F., . . . Yang, L. (2016). Visible-light-activated bactericidal functions of carbon "Quantum" dots. *ACS applied materials & interfaces, 8*(17), 10761-10766.

Miao, S., Liang, K., Zhu, J., Yang, B., Zhao, D., & Kong, B. (2020). Hetero-atom-doped carbon dots: Doping strategies, properties and applications. *Nano Today, 33*, 100879.

Neal, A. L. (2008). What can be inferred from bacterium–nanoparticle interactions about the potential consequences of environmental exposure to nanoparticles? *Ecotoxicology, 17*(5), 362-371.

Oakley, M. S., & Klobukowski, M. (2018). ΔDFT/MIX: A reliable and efficient method for calculating core electron binding energies of large molecules. *Journal of Electron Spectroscopy and Related Phenomena, 227*, 44-50.

Ogilby, P. R., & Foote, C. S. (1983). Chemistry of singlet oxygen. 42. Effect of solvent, solvent isotopic substitution, and temperature on the lifetime of singlet molecular oxygen (1. DELTA. g). Journal of the American Chemical Society, 105(11), 3423-3430.

Okimoto, Y., Watanabe, A., Niki, E., Yamashita, T., & Noguchi, N. (2000). A novel fluorescent probe diphenyl-1-pyrenylphosphine to follow lipid peroxidation in cell membranes. *FEBS letters, 474*(2-3), 137-140.

Park, I.-K., & Kang, D.-H. (2013). Effect of electropermeabilization by ohmic heating for inactivation of Escherichia coli O157: H7, Salmonella enterica serovar Typhimurium, and Listeria monocytogenes in

buffered peptone water and apple juice. *Applied and environmental microbiology, 79*(23), 7122-7129.

Prandi, B., Faccini, A., Lambertini, F., Bencivenni, M., Jorba, M., Van Droogenbroek, B., . . . Elst, K. (2019). Food wastes from agrifood industry as possible sources of proteins: A detailed molecular view on the composition of the nitrogen fraction, amino acid profile and racemisation degree of 39 food waste streams. *Food chemistry, 286*, 567-575.

Prasannan, A., & Imae, T. (2013). One-pot synthesis of fluorescent carbon dots from orange waste peels. *Industrial & Engineering Chemistry Research, 52*(44), 15673-15678.

Rabe, D. I. A., Al Awak, M. M., Yang, F., Okonjo, P. A., Dong, X., Teisl, L. R., . . . Sun, Y.-P. (2019). The dominant role of surface functionalization in carbon dots' photo-activated antibacterial activity. *International Journal of Nanomedicine, 14*, 2655.

Rodgers, M. A. (1983). Time resolved studies of 1.27 μm luminescence from singlet oxygen generated in homogeneous and microheterogeneous fluids. Photochemistry and Photobiology, 37(1), 99-103.

Scopes, R. K. (2001). Enzyme activity and assays. *e LS*.

Shahraki, H. S., Ahmad, A., & Bushra, R. (2022). Green carbon dots with multifaceted applications–Waste to wealth strategy. *FlatChem, 31*, 100310.

Shi, H., Wang, C., Wang, W., Hu, X., Fan, J., & Tang, Z. (2021). The enhanced visible light driven photocatalytic inactivation of Escherichia coli with Z-Scheme Bi2O3/Bi2MoO6 heterojunction and mechanism insight. *Ceramics International, 47*(6), 7974-7984.

Song, Z., Quan, F., Xu, Y., Liu, M., Cui, L., & Liu, J. (2016). Multifunctional N, S co-doped carbon quantum dots with pH-and thermo-dependent switchable fluorescent properties and highly selective detection of glutathione. *Carbon, 104*, 169-178.

Skovsen, E., Snyder, J. W., Lambert, J. D., & Ogilby, P. R. (2005). Lifetime and diffusion of singlet oxygen in a cell. The Journal of Physical Chemistry B, 109(18), 8570-8573.

Tavares, A., Carvalho, C., Faustino, M. A., Neves, M. G., Tomé, J. P., Tomé, A. C., . . . Alves, E. (2010). Antimicrobial photodynamic therapy: study of bacterial recovery viability and potential development of resistance after treatment. *Marine drugs, 8*(1), 91-105.

Tripathi, K. M., Ahn, H. T., Chung, M., Le, X. A., Saini, D., Bhati, A., . . . Kim, T. (2020). N, S, and P-co-doped carbon quantum dots: Intrinsic

peroxidase activity in a wide pH range and its antibacterial applications. *ACS Biomaterials Science & Engineering, 6*(10), 5527-5537.

Tyutrin, A., Wang, R., & Martynovich, E. (2022). Luminescent properties of carbon quantum dots synthesized by microplasma method. *Journal of Luminescence, 246*, 118806.

Tzeng, J.-H., Weng, C.-H., Yen, L.-T., Gaybullaev, G., Chang, C.-J., de Luna, M. D. G., & Lin, Y.-T. (2021). Inactivation of pathogens by visible light photocatalysis with nitrogen-doped TiO2 and tourmaline-nitrogen co-doped TiO2. *Separation and Purification Technology, 274*, 118979.

Vilariño, M. V., Franco, C., & Quarrington, C. (2017). Food loss and waste reduction as an integral part of a circular economy. *Frontiers in environmental science, 5*, 21.

Wang, C., Chang, T., Yang, H., & Cui, M. (2014). Surface physiological changes induced by lactic acid on pathogens in consideration of pKa and pH. *Food Control, 46*, 525-531.

Wang, H.-X., Xiao, J., Yang, Z., Tang, H., Zhu, Z.-T., Zhao, M., . . . Zhang, H.-L. (2015). Rational design of nitrogen and sulfur co-doped carbon dots for efficient photoelectrical conversion applications. *Journal of Materials Chemistry A, 3*(21), 11287-11293.

Wang, T., Liu, X., Ma, C., Zhu, Z., Liu, Y., Liu, Z., . . . Huo, P. (2018). Bamboo prepared carbon quantum dots (CQDs) for enhancing Bi3Ti4O12 nanosheets photocatalytic activity. *Journal of Alloys and Compounds, 752*, 106-114.

Wei, Y., Chen, L., Zhao, S., Liu, X., Yang, Y., Du, J., . . . Yu, S. (2021). Green-emissive carbon quantum dots with high fluorescence quantum yield: Preparation and cell imaging. *Frontiers of Materials Science, 15*(2), 253-265.

Xia, D., Shen, Z., Huang, G., Wang, W., Yu, J. C., & Wong, P. K. (2015). Red phosphorus: an earth-abundant elemental photocatalyst for "green" bacterial inactivation under visible light. *Environmental science & technology, 49*(10), 6264-6273.

Yang, G., Wan, X., Su, Y., Zeng, X., & Tang, J. (2016). Acidophilic S-doped carbon quantum dots derived from cellulose fibers and their fluorescence sensing performance for metal ions in an extremely strong acid environment. *Journal of Materials Chemistry A, 4*(33), 12841-12849.

Yang, Y., Lin, X., Li, W., Ou, J., Yuan, Z., Xie, F., . . . Chi, Z. (2017). One-pot large-scale synthesis of carbon quantum dots: efficient cathode

interlayers for polymer solar cells. *ACS applied materials & interfaces*, *9*(17), 14953-14959.

Yao, X.-H., Min, H., & Lv, Z.-M. (2006). Response of superoxide dismutase, catalase, and ATPase activity in bacteria exposed to acetamiprid. *Biomedical and Environmental Sciences*, *19*(4), 309.

Yi, J., Huang, K., Young, G. M., & Nitin, N. (2020). Quantitative analysis and influences of contact dynamics on bacterial cross-contamination from contaminated fresh produce. *Journal of Food Engineering*, *270*, 109771.

Yoon, D. S., Lee, M.-H., & Cha, D. S. (2018). Measurement of intracellular ROS in Caenorhabditis elegans using 2', 7'-dichlorodihydrofluorescein diacetate. *Bio-protocol*, *8*(6), e2774-e2774.

Yu, Y., Xu, W., Fang, J., Chen, D., Pan, T., Feng, W., . . . Fang, Z. (2020). Soft-template assisted construction of superstructure TiO2/SiO2/g-C3N4 hybrid as efficient visible-light photocatalysts to degrade berberine in seawater via an adsorption-photocatalysis synergy and mechanism insight. *Applied Catalysis B: Environmental*, *268*, 118751.

Zhang, C., Li, Y., Shuai, D., Shen, Y., Xiong, W., & Wang, L. (2019). Graphitic carbon nitride (g-C3N4)-based photocatalysts for water

disinfection and microbial control: A review. *Chemosphere, 214*, 462-479.

Zhang, C., Li, Y., Shuai, D., Zhang, W., Niu, L., Wang, L., & Zhang, H. (2018). Visible-light-driven, water-surface-floating antimicrobials developed from graphitic carbon nitride and expanded perlite for water disinfection. *Chemosphere, 208*, 84-92.

Zhang, Y., Yang, C., Yang, D., Shao, Z., Hu, Y., Chen, J., . . . Wang, L. (2018). Reduction of graphene oxide quantum dots to enhance the yield of reactive oxygen species for photodynamic therapy. *Physical Chemistry Chemical Physics, 20*(25), 17262-17267.

Zhu, C., Zhai, J., & Dong, S. (2012). Bifunctional fluorescent carbon nanodots: green synthesis via soy milk and application as metal-free electrocatalysts for oxygen reduction. *Chemical communications, 48*(75), 9367-9369.

VI. 국문초록

이 연구의 목적은 커피 찌꺼기 (SCG)를 바이오매스로 사용하여 가시광선유래 (VLD) 항균활성을 나타내는 탄소 양자점 (CQD) 을 합성하는 것이다. CQD 는 마이크로파 처리를 통해 SCG 에서 합성되었으며. 고해상도 투과 전자 현미경, 동적 광산란, X 선 광전자 분광법 분석을 통해 적절한 CQD 가 합성되었음을 확인하였다. SCG 에서 합성한 CQD 의 *Escherichia coli* O157:H7 에 대한 VLD 항균 활성은 pH 가 감소함에 따라 증가하는 것으로 밝혀졌다. VLD 항균 활성과 관련된 CQD 의 광역학적 특성인 형광양자수율, 밴드갭에너지 및 형광수명은 pH 변화에 따른 유의한 변화를 나타내지 않았다. 한편, pH 가 감소함에 따라 CQD 와 병원성 세균의 음의 제타전위(mV) 값은 점차 감소하였다. 그 결과, *E. coli* O157:H7 에 대한 CQD 흡수는 그들 사이의 반발력의 감소로 인해 점진적으로 증가함을 확인하였다. 또한, pH 가 감소할수록 세포 내 활성산소(ROS)를 소거하는 것으로 알려진 효소 (과산화물 디스뮤타제 및 카탈라제)의 활성이 감소함을 알 수 있었다. CQD 존재 하에서 가시광선을 조사했을 때

pH 가 감소함에 따라 세포 내부에서 생성된 ROS 의 양이 증가하였다.

나아가 CQD 의 VLD 항균 활성은 사과세척에 적용되었다. CQD 를 이용한 VDL 항균처리로 사과와 CQD 용액 모두에서 *E. coli* O157:H7 의 유의적인 감소 ($P < 0.05$)가 발생했으며 교차오염도 방지되었다. CQD 의 활성은 3 회 연속처리 주기 동안 재사용 후에도 유지되었으며, 4 주 동안 CQD 의 제조일자별 활성에는 차이가 없었다 ($P > 0.05$).

본 연구의 결과는 산성조건에서 SCG 에서 합성된 CQD 를 사용하는 것이 유리하고 신선농산물 세척공정에 CQD 기반 VDL 항균활성의 적용가능성을 제시한다. 본 연구에 따라 pH 조건에 영향을 받지 않는 CQD 합성방법에 대한 추가연구가 필요하다.

주요어: **탄소양자점, 가시광선, 병원성대장균, 미생물 저감화, 저감화 기작, 신선 식품 세척**

학번: 2021-27817